

Wilfrid Laurier University

Scholars Commons @ Laurier

---

Theses and Dissertations (Comprehensive)

---

2024

## Synthesis and Biophysical Analysis of Modified Cell-Penetrating Peptides

Joel Mitchell  
mitc2080@mylaurier.ca

Follow this and additional works at: <https://scholars.wlu.ca/etd>



Part of the [Biochemistry Commons](#), and the [Biophysics Commons](#)

---

### Recommended Citation

Mitchell, Joel, "Synthesis and Biophysical Analysis of Modified Cell-Penetrating Peptides" (2024). *Theses and Dissertations (Comprehensive)*. 2594.

<https://scholars.wlu.ca/etd/2594>

This Thesis is brought to you for free and open access by Scholars Commons @ Laurier. It has been accepted for inclusion in Theses and Dissertations (Comprehensive) by an authorized administrator of Scholars Commons @ Laurier. For more information, please contact [scholarscommons@wlu.ca](mailto:scholarscommons@wlu.ca).

# **Synthesis and Biophysical Analysis of Modified Cell-Penetrating Peptides**

By

Joel Mitchell

Honours BSc Biochemistry and Biotechnology, Wilfrid Laurier  
University, December 2020

THESIS

Submitted to the Department of Chemistry and Biochemistry  
Faculty of Science

in partial fulfillment of the requirements for the  
Master of Science in Chemistry  
Wilfrid Laurier University

2023

Joel Mitchell 2023©

## Abstract

Cell-penetrating peptides (CPPs) are a family of peptides that have the ability to penetrate biological membranes. They were discovered in the late 1980s and have been the topic of many studies. Much of the interest in CPPs has been due to their ability to translocate biological membranes, and the possibility that they could offer a novel drug delivery method by conjugation to biologically active molecules. Linear CPPs can be modified to form cyclic structures. This change in structure has been observed to enhance the stability and penetrative ability of the CPPs which have been studied. The current thesis focuses on the biophysical properties of CPPs modified to allow for cyclization. Penetratin (primary sequence: RQIKIWFQNRRMKWKK) and the Tat peptide (primary sequence: YGRKKRRQRRR) are two examples of linear CPPs that interact with and translocate across biological membranes. Fmoc based solid-phase peptide synthesis (SPPS) was used to synthesize cyclizable analogs of these two peptides by adding glycine and cysteine residues to the peptides' termini. Reversed-phase high performance liquid chromatography (RP-HPLC) was used to purify and analyze the homogeneity of the protected linear analogs of the Tat peptide and penetratin (pTatL and pPenL, respectively). Fluorescence emission spectroscopy and circular dichroism (CD) spectroscopy were used to observe the conformational differences between the cyclizable analogs, and their original peptide constructs in different (aqueous, organic solvent and lipidic) environments. Dithiothreitol was required to measure the fluorescence and CD spectra of the peptides in the presence of lipid vesicles, to prevent the precipitation which might occur in the absence of the reducing agent. The CD and fluorescence spectra of pPenL were similar to the previously reported spectra of the native penetratin peptide; it displayed an unordered conformation in aqueous environments and  $\alpha$ -helical conformations in organic solvents hexafluoroisopropanol and lipidic phosphatidylcholine/phosphatidylglycerol and phosphatidylethanolamine/phosphatidylglycerol (PC/PG and PE/PG) environments. The Tat peptide has been reported to maintain an unordered secondary structure in all environments and when conjugated to biologically active molecules. The spectra of pTatL in aqueous buffer agreed with the previous reports, but the spectra in HFIP displayed partial  $\alpha$ -helical conformations, likely due to the modifications made to the sequence to enable cyclization.

## Acknowledgements

I would like to begin by thanking my supervisors, Dr. Masoud Jelokhani-Niaraki and Dr. Matthew Smith for inviting me into their lab group as a summer NSERC-USRA student; without that invitation and push I would have never joined this amazing lab group and this research study would have never come to fruition. I am very thankful to have been a part of this group as an undergraduate student and later as a graduate student. Having Dr. Jelokhani and Dr. Smith has not only helped open my eyes to new ways of thinking and approaching difficult research tasks but has also helped me develop hands on skills using many different types of instrumentation that I may not have had the opportunity to use if I were to have joined another group. I am very appreciative for all the time (and money) you two have spent teaching and troubleshooting while working with me throughout the years. I am not sure what exactly my next adventure in the world of science will look like, but I know that I will have the information and lessons from your teaching to help guide me along the way.

I would also like to thank all my lab members, past and present: Afshan, An, Habib, Mike, Marzieh, George, Elizabeth, Ceaira, Aaron, Noah, and any others that I have spent time within the lab throughout the years. I wouldn't have been able to make it this far without your friendship and willingness to help troubleshoot/bounce ideas off. Special thank you to An and George for assistance with some of the materials used throughout this project.

Similarly, I would like to thank my friends and colleagues in the science research building who have been there for me at all hours of the day and night. Whenever I may have needed a break, a second (or third) set of eyes you were there.

I would like to thank Joe Meissner for giving me the opportunity to IA and TA a wide range of biochemistry labs, some that I wasn't sure that I was qualified to help teach. As one of the students in your lab and as someone assisting you teach the lab, you always provided a safe, productive and fun space for all. And thank you for allowing us to use your lab space during the Summer 2023 Science Research renovations!

Finally, I would like to thank the rest of the Chemistry and Biochemistry department. I have learned so much from you inside and outside of the classrooms. I thank you all for being so approachable whether it be for course related questions, research related questions, or just general conversation.

This MSc study was partially funded by 2021 Ontario Graduate Scholarship (OGS), the Department of Chemistry, the Faculty of Graduate and Postdoctoral Studies, and my supervisors.

## **Declaration of Work Performed**

I declare that I am the sole author of this thesis project, which includes all the lab experiments (unless otherwise stated in the document) and this written thesis. I personally synthesized the peptide analogs used in this project, with the exception of the Pen2 peptide which had previously been synthesized by An Le, a previous graduate student. All the CD and fluorescence experiments were performed a minimum of two times to ensure that the results were reproducible.

## Table of Contents

Abstract.....	i
Acknowledgements .....	ii
Declaration of Work Performed.....	iii
List of Figures .....	v
List of Tables .....	vi
Abbreviations.....	vi
<b>Chapter 1: Introduction</b> .....	<b>1</b>
<b>1.1 Cell-Penetrating Peptides</b> .....	<b>1</b>
<b>1.2 Tat and Tat Peptide Analogs</b> .....	<b>4</b>
<b>1.3 Homeoproteins and Penetratin</b> .....	<b>6</b>
<b>1.4 Biological Membranes</b> .....	<b>7</b>
<b>1.5 Studies related to the penetratin and Tat peptides and their cyclic analogs</b> .....	<b>11</b>
<b>1.6 Objectives of the Research</b> .....	<b>13</b>
<b>Chapter 2: Materials and Methods</b> .....	<b>15</b>
<b>2.1 Methods and Techniques</b> .....	<b>16</b>
2.1.1 Solid Phase Peptide Synthesis .....	16
2.1.2 Peptide Cyclization .....	19
2.1.3 Peptide Purification.....	22
2.1.4 Lipid Vesicle Preparation .....	23
2.1.5 Circular Dichroism Spectroscopy .....	23
2.1.6 Fluorescence Spectroscopy.....	25
2.1.7 Isothermal Titration Calorimetry .....	28
<b>2.2 Materials and Experimental Procedures</b> .....	<b>29</b>
2.2.1 Solid Phase Peptide Synthesis .....	29
2.2.2 Peptide Purification.....	33
2.2.3 Lipid Vesicle Preparation .....	36
2.2.4 Circular Dichroism Spectroscopy .....	36
2.2.5 Fluorescence Spectroscopy.....	37
2.2.6 Isothermal Titration Calorimetry .....	38
<b>Chapter 3: Results and Discussion</b> .....	<b>39</b>
<b>3.1 Synthesis and Purification of the Cell-Penetrating Peptides</b> .....	<b>39</b>

<b>3.2 Use of Dithiothreitol in sample preparation and vesicle preparation</b> .....	46
<b>3.3 Fluorescence Emission</b> .....	48
3.3.1 pTatL fluorescence in different environments .....	48
3.3.2 pPenL fluorescence in different environments .....	50
3.3.3 Effect of cysteine on the fluorescence emission of penetratin analogs .....	52
3.3.4 Effect of fluorine on the fluorescence emission.....	55
<b>3.4 Circular Dichroism Spectroscopy</b> .....	58
3.4.1 pTatL in different environments .....	58
3.4.2 pPenL in different environments.....	61
<b>3.5 Isothermal Titration Calorimetry</b> .....	63
<b>Chapter 4: Conclusions</b> .....	64
<b>References</b> .....	67
<b>Appendix</b> .....	72

## List of Figures

Figure 1-1. Proposed mechanisms of CPP uptake.....	4
Figure 1-2. A visual breakdown of the three major lipid types that can be found in biological membranes and their components.....	8
Figure 1-3. The general structure and characteristics of common phospholipids.....	10
Figure 2-1. A basic overview of Fmoc based solid-phase synthesis (SPPS).....	18
Figure 2-2. The stepwise process of on-resin cyclization via disulfide bond formation.....	21
Figure 2-3. CD spectra of protein backbone corresponding to common secondary structures.....	25
Figure 2-4. A Jablonksi diagram demonstrating the mechanism of fluorescence.....	26
Figure 2-5. Flow-chart for selecting the appropriate cleavage cocktail for Fmoc SPPS based on peptide sequence.....	33
Figure 3-1. Analytical and semipreparative RP-HPLC chromatograms of pTatL through the purification process.....	43
Figure 3-2. Analytical and semipreparative RP-HPLC chromatograms of pPenL through the purification process.....	45

Figure 3-3. Peptide-lipid vesicle mixtures in the presence and absence of dithiothreitol (DTT)..	48
Figure 3-4. Fluorescence spectra of varying concentrations of pTatL in buffer and 50% HFIP and buffer.....	50
Figure 3-5. Fluorescence spectra of varying concentrations of pPenL in different environments excited at 280 nm.....	52
Figure 3-6. Fluorescence spectra of varying concentrations of pPenL and Pen2 in buffer excited at 280 nm.....	54
Figure 3-7. Fluorescence spectra of varying concentrations of pPenL and Pen2 in PC/PG and PE/PG lipid systems excited at 280 nm.....	55
Figure 3-8. Fluorescence spectra of varying concentrations of pPenL in different buffer and organic environments to observe the effect of fluoride and fluorinated alcohols.....	57
Figure 3-9. Fluorescence spectra of L-tryptophan in buffer and 50% HFIP and buffer.....	58
Figure 3-10. CD spectra of pTatL in buffer in the absence and presence of 50% HFIP.....	60
Figure 3-11. CD spectra of pPenL at different concentrations in buffer environments (buffer with and without 50% HFIP) and in the presence of lipid vesicles and lipid vesicle mimics (PC/PG, PE/PG, and 50% HFIP).....	62

## List of Tables

Table 2-1. Experimental methods and the corresponding biologically relevant environments.....	15
Table 2-2. Isothermal Titration Calorimetry measurement conditions.....	39
Table 3-1. Penetratin and Tat peptide analogs used for this study.....	46

## Abbreviations

- aa – Amino Acid
- AcCN – Acetonitrile
- CD – Circular Dichroism Spectroscopy
- CPPs – Cell-Penetrating Peptides
- DCM – Dichloromethane or Methylene chloride
- DIPEA – N,N-Diisopropylethylamine
- DLS – Dynamic Light Scattering
- DMF – N,N'-Dimethylformamide

- DPH – 1,6-Diphenyl-1,3,5-hexatriene
- DTNP – 2,2'-Dithiobis(5-nitropyridine)
- EDT – Ethanedithiol
- ESI-MS – Electrospray ionization mass spectrometry
- Fmoc – fluorenyl methoxy carbonyl
- HCTU – 1H-benzotriazolium 1-[bis(dimethylamino)methylene]-5-chloro-hexafluorophosphate (1-), 3-oxide
- HFIP – Hexafluoro-2-propanol or Hexafluoroisopropanol
- HOBt – 1-hydroxybenzotriazole
- IsoP – Isopropanol
- ITC – Isothermal Titration Calorimetry
- LUV – Large Unilamellar Vesicles (or Liposomes)
- Mmt – 4-methoxytrityl
- MRE – Mean residue ellipticity
- NMP – N-Methylpyrrolidone
- PC – Phosphatidylcholine
- PE – Phosphatidylethanolamine
- PG – Phosphatidylglycerol
- PI – Phosphatidylinositol
- POPC – 1-palmitoyl-2-oleoyl-sn-3-glycero-phosphatidylcholine
- POPE – 1-palmitoyl-2-oleoyl-sn-3-glycerophosphatidylethanolamine
- POPG – 1-palmitoyl-2-oleoyl-sn-3-glycero-phosphatidylglycerol
- PS – Phosphatidylserine
- PTD – Peptide transduction domain
- p-TEFb – Positive transcription elongation factor b
- RP-HPLC – Reverse-Phase High Performance Liquid Chromatography
- SM – Sphingomyelin
- SPPS – Solid Phase Peptide Synthesis
- S-t-Bu – tert-butylthio
- TFA – Trifluoroacetic acid
- TFE – Trifluoroethanol
- TIS – Triisopropylsilane
- TMA-DPH – 1-(4-Trimethylammoniumphenyl)-6-Phenyl-1,3,5-Hexatriene p-Toluene sulfonate

# Chapter 1: Introduction

## 1.1 Cell-Penetrating Peptides

Cell-penetrating peptides (CPPs) are a family of peptides that can penetrate cellular membranes, as the name suggests. They are sometimes referred to as peptide transduction domains (PTDs) and are generally short, cationic peptides consisting of 4-40 amino acids.<sup>1</sup> CPPs were first discovered in the late 1980s, when scientists identified proteins that could enter cells by crossing their plasma membranes, without assistance of any external machinery. This was a major finding as it was previously assumed that the plasma membranes were impermeable to hydrophilic molecules.<sup>2</sup> Many potential applications for CPPs have been suggested given their unique abilities to translocate across biological membranes. Some of these applications include using a CPP to carry biologically active substances such as drugs, small interfering RNA (siRNA) or other proteins and peptides across membranes.<sup>1-3</sup> It has been suggested that some CPPs also may have direct applications as antimicrobial, antifungal, or antibacterial agents.<sup>3</sup>

CPPs have been extensively researched since their discovery, with hundreds of peptides being studied and classified into multiple proposed groups. Some of the more common characteristics used to classify CPPs are whether they are protein-derived *vs* designed, physicochemical properties *vs* structural properties and having linear *vs* cyclic structures.<sup>1</sup> The latter categorization will be one of the main inspirations of this thesis research.

Cyclic peptides, are single peptide or polypeptide chains present in a ring structure.<sup>4-6</sup> The ring structure can be formed in different ways, such as through an amide bond linking one end of the peptide to another or other chemically stable bonds.<sup>4</sup> A popular method used to form cyclic peptides is through the formation of disulfide bonds.<sup>5,6</sup> Cyclic peptides have become very popular

in the world of drug design, as studies have shown that cyclic peptides display better biological activity than linear peptides thanks to their conformational rigidity.<sup>4,5</sup> Cell permeability is enhanced using cyclic peptides as the overall polarity and hydrogen bonding are reduced by stabilizing peptides in optimal conformations for interacting with the target membranes.<sup>4,5</sup> The metabolic stability of linear peptides to enzymatic hydrolysis is also enhanced by cyclization.<sup>5</sup>

Since there are CPPs that can fit into multiple classes, it would be logical to assume that there are different mechanisms by which CPPs are able to penetrate biological membranes. Two major mechanisms have been reported in the literature, endocytic pathways and nonendocytic pathways also known as membrane translocation pathways.<sup>3,7,8</sup>

Nonendocytic pathways are energy-independent pathways; the most common nonendocytic uptake mechanism of CPPs is direct penetration.<sup>7</sup> Direct penetration is an energy-independent pathway which relies on a positively charged CPP interacting with the negatively charged components of a membrane to initiate the translocation process.<sup>3,7-9</sup> Direct penetration mechanisms result from the destabilization of the membrane by the folding of the peptide on the lipid membrane.<sup>7</sup> This type of uptake mechanism is most probable for primary amphipathic CPPs at high concentrations.<sup>7</sup> Examples of different forms of direct penetration include the carpet-like model, pore formation, inverted micelle formation and the membrane thinning model.<sup>7</sup>

Unlike direct penetration, endocytosis is an energy-dependent pathway. Energy is often required for macromolecules to traverse the cellular membranes; endocytosis is the active pathway in which said macromolecules are carried into the cells.<sup>7,8</sup> Endocytosis is sometimes referred to as cell digestion as the plasma membrane engulfs the CPP and absorbs it.<sup>3</sup> A portion of the membrane surrounds the CPP, forming a vesicle which is taken into the cell.<sup>3</sup> Literature suggests that peptides in lower concentrations, or when conjugated to cargo, are taken up by cells via endocytosis.<sup>7,8</sup>

Endocytosis can be further divided into three main classes: pinocytosis, phagocytosis and receptor-mediated endocytosis.<sup>3,7,8,10</sup> Two distinct steps are involved in all of these classes of endocytosis, an endocytic uptake step followed by endosomal escape.<sup>8</sup>

A general visual representation of the two proposed mechanisms in which CPPs cross biological membranes is shown in Figure 1-1.

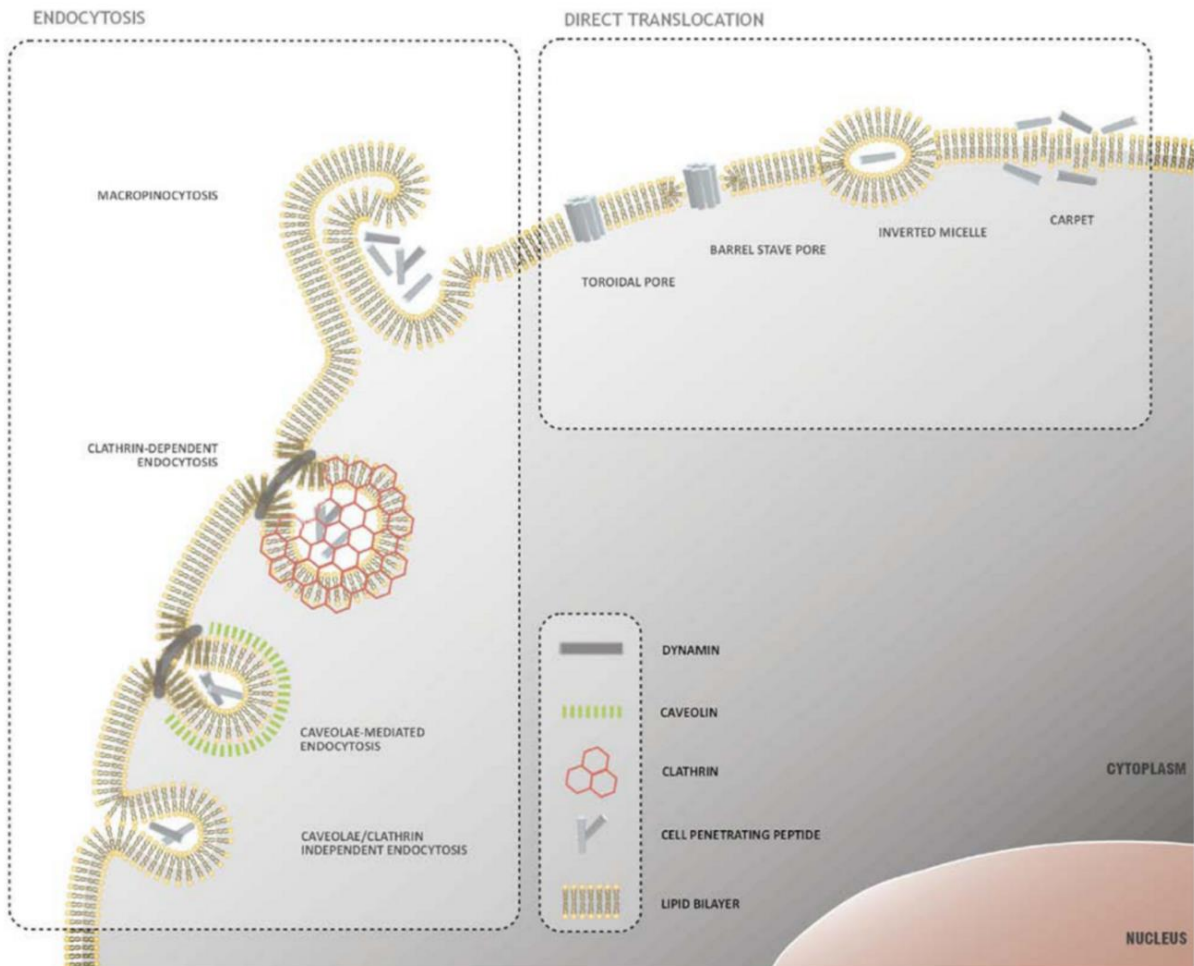


**Figure 1-1. Proposed mechanisms of CPP uptake.**

Two main mechanisms have been proposed for the uptake of CPPs into the cell: direct translocation through the cell membrane and endocytosis. Direct translocation mechanisms require no energy and include mechanisms such as pore formation, inverted micelle, and the carpet model. Endocytosis mechanisms are energy-dependent processes which include micropinocytosis, clathrin-dependent endocytosis, caveolae-mediated endocytosis and caveolae/clathrin independent endocytosis. This figure was taken from Reference 8 where it can be seen as Figure 1, copyright Trabulo et al., 2010. CC-BY 3.0 (<https://creativecommons.org/licenses/by/3.0/>).<sup>8</sup>

## 1.2 Tat and Tat Peptide Analogs

In 1988, two independent research groups, who were working with the trans-activating transcriptional activator (Tat) from Human Immunodeficiency Virus 1 (HIV-1), discovered that

this protein could be efficiently taken up by numerous cell types *in vitro*.<sup>1,11,12</sup> This finding led to studies trying to determine which part(s) of the protein was (were) important for the translocation across the biological membranes. These studies resulted in the discovery of the first CPP, known as Tatp.<sup>11</sup> Tatp is composed of residues 37-72 of the parent 86 aa Tat protein. This stretch of amino acids corresponded to the basic domain (residues 49-57) as well as an amphipathic  $\alpha$ -helical region (residues 38-49).<sup>11</sup> It was initially thought that the  $\alpha$ -helical region was the most important section for Tat protein transduction, but it was later found that the basic domain was the required component.<sup>11,13,14</sup> As a result of numerous studies, the generally accepted Tat CPP is made up of residues 47-57 (<sup>47</sup>YGRKKRRQRRR<sup>57</sup>).<sup>11</sup> This linear peptide can be converted to a cyclized form if a cysteine and a glycine are added to each terminus (CGYGRKKRRQRRRGC). This modified sequence is one of the peptides studied in this research project. The exact mechanism by which the Tat peptide crosses membranes is not known; it was originally suggested that the peptide enters cells using energy-dependent pathways, but more recent findings suggest that Tat utilizes an energy-independent endocytosis pathway.<sup>15</sup>

As mentioned above, Tat peptide was derived from the trans-activating transcriptional activator of HIV-1. HIV-1 Tat is one of the first proteins to be expressed after HIV infection takes place.<sup>12,16</sup> It is crucial in regulating transcription, but unlike other transcription factors the protein binds to RNA instead of DNA.<sup>16</sup> Once bound to the target RNA, the HIV-1 Tat protein recruits the host positive transcription elongation factor b (p-TEFb).<sup>16</sup> This enhances the activity of RNA Polymerase II complexes which is necessary for the elongation of the viral transcripts.<sup>16</sup> The PTD of the HIV-1 Tat protein allows the protein to cross biological membranes including cell membranes, the blood brain barrier and the nuclear membranes.<sup>12,16,17</sup> The HIV-1 virus was first isolated in 1983, but it took another three years (1986) to discover the protein for regulating

transcription. Two years later (1988) the sequence of the protein responsible for translocation was determined.

### 1.3 Homeoproteins and Penetratin

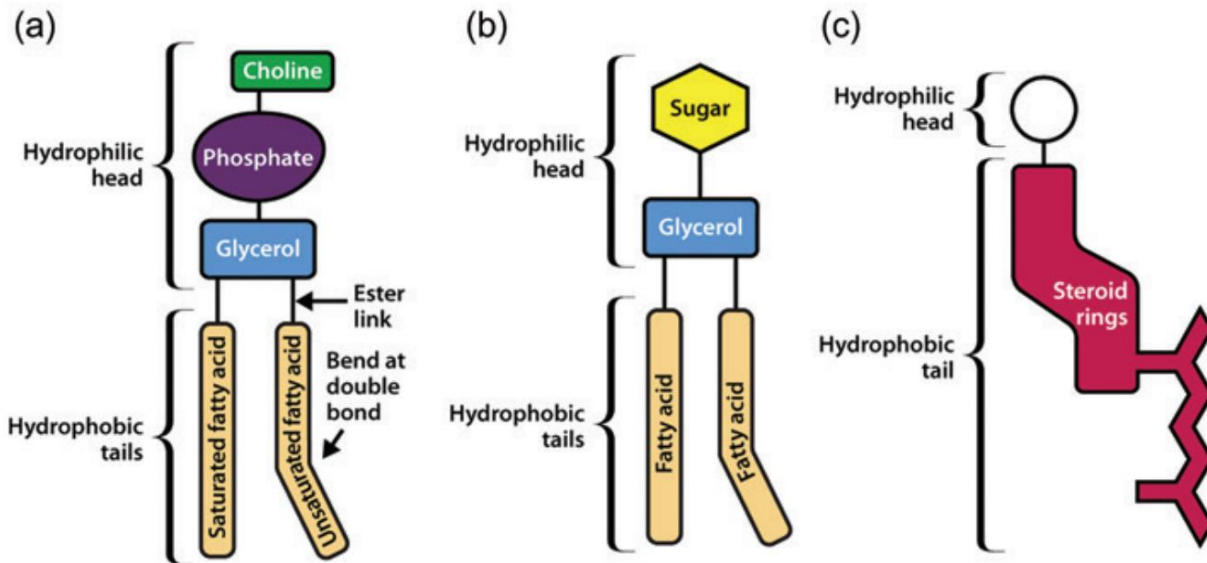
In 1994, the same year that it was discovered that only a portion of the Tat protein was necessary for cellular uptake, it was found that another short amino acid sequence of a larger protein was necessary and sufficient for cellular uptake.<sup>1,11</sup> A 16 amino acid peptide, now known as penetratin, was derived from the 60 aa homeodomain of Antennapedia, which is a homeoprotein in *Drosophila*.<sup>1</sup> The sequence of penetratin was derived from the third  $\alpha$ -helix of the homeodomain, consisting of residues 43-58 (<sup>43</sup>RQIKIWFQNRRMKWKK<sup>58</sup>).<sup>1,11</sup> The mechanism by which penetratin is able to cross biological membranes varies depending on the environment, peptide concentration and the membrane composition, but it has been suggested in literature that penetratin can penetrate the membranes via direct translocation (direct penetration) and by endocytosis.<sup>7,18</sup> Penetratin's primary sequence implies the formation of an  $\alpha$ -helix, but it has not been found to take on this structure on its own unless it is in the presence of anionic lipids.<sup>15,19</sup> In buffer, the peptide has been found to have a random structure, but once interacting with the anionic lipids in the membrane it forms an  $\alpha$ -helix.<sup>15</sup> This change in conformation is common among many amphipathic CPPs like penetratin.<sup>15</sup>

Many of the protein-derived CPPs are derived from a family of proteins known as homeoproteins. Homeoproteins are transcription factors, which are important for initiating and regulating the transcription of DNA into RNA. They are defined as any protein containing a homeodomain. A homeodomain is a 60 amino acid DNA-binding domain which is composed of three  $\alpha$ -helices with the third playing a crucial role in the binding of the homeoprotein to its binding

site.<sup>18,20</sup> Homeoproteins were first discovered in flies (*Drosophila*) but have since been found in all metazoans and in plants.<sup>20</sup> Penetratin was derived from the homeodomain of Antennapedia, a homeoprotein found in *Drosophila*. Antennapedia functions as a transcription factor regulating the second thoracic region in *Drosophila*, determining whether second legs or antennae are formed.<sup>21</sup>

#### 1.4 Biological Membranes

Biological membranes are essential for life. They act as barriers for cells and organelles protecting their contents from harmful conditions in the surrounding environment, while allowing the exchange of necessary substances. Biological membranes consist of a bilayer of lipid molecules, which is often referred to as a phospholipid bilayer.<sup>22</sup> The membrane is also composed of a network of proteins, known as membrane proteins, and different sugars covalently attached to lipids or proteins. The majority of lipids that make up the membrane are phospholipids, but there can also be sterols and glycolipids.<sup>22</sup> Phospholipids are made up of two fatty acid chains connected to a glycerol which is also connected to a phosphate group, as seen in Figure 1-2a.<sup>22</sup> A unique type of phospholipid that is mainly found in eukaryotic membranes are sphingolipids. They have similar structures to phospholipids except they contain a sphingosine backbone instead of glycerol. Glycolipids are similar to phospholipids except the phosphate group is replaced by a sugar, Figure 1-2b.<sup>22</sup> Sterols are most commonly found in eukaryotes, they consist of a sterol ring connected to a hydroxyl group on one part and a carbon chain on another.<sup>22</sup>

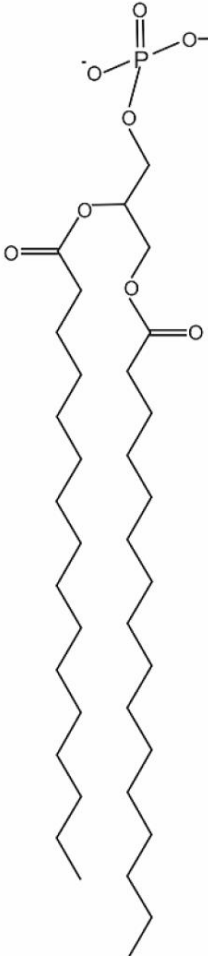
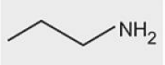
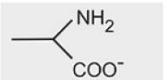
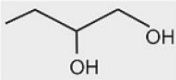
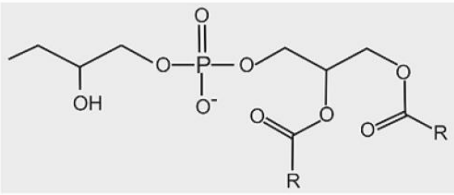
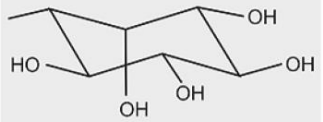


**Figure 1-2: A visual breakdown of the three major lipid types that can be found in biological membranes and their components.**

(a) represents a phospholipid with two fatty acids making up the hydrophobic tails and glycerol, phosphate and another group attached to the phosphate making up the hydrophilic head; this specific example is of phosphatidylcholine. (b) represents a glycolipid, it has a similar makeup to that of a phospholipid except the phosphate group is replaced by a sugar. (c) represents a sterol with the steroid rings and the hydrocarbon chain making up the hydrophobic tail and the hydroxyl group as the hydrophilic head. This figure was taken from Reference 22, with permission, where it can be seen as Figure 1.<sup>22</sup>

Some of the common phospholipid structures are depicted in Figure 1-3. Not all phospholipids are found in each membrane, and the two layers of the membranes are often asymmetric as certain phospholipids tend to favour either the inner or the outer leaflets. For example, phosphatidylcholine (PC), phosphatidylethanolamine (PE), phosphatidylserine (PS), and sphingomyelin (SM) are four of the major phospholipids found in animal cells.<sup>23</sup> Of these four lipids, PC and SM prefer the outer leaflet, whereas PE and PS prefer the inner leaflet of plasma membranes.<sup>23,24</sup>

Unilamellar lipid vesicles are commonly used as model biological membranes.<sup>25</sup> They are in vitro derived lipid bilayers that are generally made of a mixture of phospholipids. They can be made in a variety of sizes; small unilamellar vesicles (SUVs) range from 10-100 nm in diameter, large unilamellar vesicles (LUVs) generally range from 100-500 nm in diameter, and giant unilamellar vesicles (GUVs) are greater than 1  $\mu\text{m}$  in diameter.<sup>25</sup> Unilamellar lipid vesicles can help us to understand how biologically active molecules interact with membranes of different compositions as well as to visualize the form and function of said molecules within a bilayer environment.

Basic phospholipid structure	Substituent (X)	Phospholipid/Characteristic
		<b>hydrogen</b> <b>PA</b> <b>anionic</b>
		<b>ethanolamine</b> <b>PE</b> <b>zwitterionic</b>
		<b>choline</b> <b>PC</b> <b>zwitterionic</b>
		<b>serine</b> <b>PS</b> <b>anionic</b>
		<b>glycerol</b> <b>PG</b> <b>anionic</b>
	 <b>phosphatidylglycerol</b>	<b>CL</b> <b>anionic</b>
		<b>inositol</b> <b>PI</b> <b>anionic</b>

**Figure 1-3: The general structure and characteristics of common phospholipids.**

The general structure of phospholipids as well as the unique headgroup structure, code and overall charge of the common phospholipids. The basic structure of a phospholipid is on the left, with the “X” representing one of the substituents in the second column. The two-letter code used to identify the phospholipid with the corresponding substituents can be seen on the right as well as their charge characteristic. This figure was taken from reference 24 where it can be seen as Figure 1, copyright Aktas et al., 2014. CC-BY 4.0. (<https://creativecommons.org/licenses/by/4.0/>).<sup>24</sup>

## 1.5 Studies related to the penetratin and Tat peptides and their cyclic analogs

As mentioned previously, the Tat peptide, which is derived from the HIV1 Tat protein, is an 11 amino acid cationic peptide (primary sequence YGRKKRRQRRR).<sup>11</sup> It was one of the first CPPs discovered; the same year that a similar CPP, penetratin, was discovered.<sup>1</sup> Penetratin was also derived from a larger protein, the homeodomain of the *Antennapedia* protein.<sup>1</sup> Like the tat peptide, penetratin is an arginine rich cationic CPP but is slightly longer, consisting of 16 amino acids (primary sequence RQIKIWFQNRRMKWKK).<sup>1</sup> Both peptides are known to interact with the cell membranes and enter the cells, though the mechanisms in which they enter are thought to be different. The tat peptide is said to enter cells using clathrin-mediated endocytosis when it is not conjugated to any molecules, but is said to utilize micropinocytosis or caveolae-mediated endocytosis when conjugated to proteins.<sup>8</sup> In low concentrations penetratin has been shown to enter cells via direct penetration, while in higher concentrations it enters the cells via endocytosis.<sup>8</sup>

The differences in the mechanism of entry of the two arginine rich, cationic CPPs could be related to their differing secondary structures.<sup>26</sup> The tat peptide has been shown to have no defined secondary structure.<sup>26,27</sup> This remains true when the peptide is conjugated to proteins and other molecules.<sup>26,27</sup> The secondary structure of penetratin, on the other hand, has been shown to be dependent on its environment.<sup>10,26</sup> Penetratin has been shown to prefer a random structure in aqueous environments, but becomes more ordered in the presence of membranes containing negatively charged phospholipids.<sup>10,26</sup> In the presence of these membranes, penetratin takes on an  $\alpha$ -helical secondary structure in lower concentrations of peptide and adopts an antiparallel  $\beta$ -sheet conformation in higher concentrations.<sup>10,26</sup>

While these two CPPs have been well-studied, not much has been reported on the mechanism of their cyclic analogs and how they compare to that of the native forms. Cyclic

peptides, as mentioned previously, have many advantages over their linear counterparts due to their more rigid and stable conformations.<sup>4,5</sup> Soo-Jin Lee and their group out of South Korea employed a common cyclization modification to the native tat peptide sequence.<sup>28</sup> The group added a cysteine residue to the N and C-termini of the peptide sequence to allow for disulfide bond formation.<sup>28</sup> A separate group working out of China, led by Jianli Ren, used a similar modification to the native tat peptide sequence to form a cyclic analog.<sup>29</sup> They formed the cyclic structure through a disulfide bond between the terminal cysteine residues, but also included a singular glycine residue between the cysteines and the native sequence (modified sequence CGYGRKKRRQRRRG).<sup>29</sup> The Korean and Chinese groups studied the difference in gene delivery efficiency of the tat peptide and its analogs, but neither published any work regarding any changes in the mechanism of penetration or their secondary structures.

Tung's group, at Harvard Medical School, proposed a method of on-resin disulfide bond formation in peptides, which provided a protocol for a more controlled cyclization method than that of the post cleavage methods.<sup>6</sup> In their proposed method, disulfide bonds are formed through cysteine residues in the peptide sequence, with specific side chain protecting groups.<sup>6</sup> *tert*-Butylthio and 4-methoxytrityl thiol protecting groups were used with the cysteines involved in the disulfide bonds in the synthesis of the target peptides.<sup>6</sup> The formation of a disulfide bond between the cysteines with these specific thiol protecting groups occurs in three steps involving two nucleophilic attacks, resulting in the cyclization of the peptide prior to cleavage from the resin used to synthesize the peptide.<sup>6</sup>

An Le, a previous graduate student in the Jelokhani-Smith lab group conducted extensive studies on the penetratin peptide, its aromatic analogs and their interaction with different environments.<sup>30</sup> These studies were done to better understand how penetratin interacts with the

lipid membranes and to observe the effect that the tryptophan residues contained in penetratin had on the interaction.<sup>30</sup> Many of the techniques utilized by Le can also be used when working with the penetratin and Tat analogs in this study; the techniques included synthesis and purification methods as well as biophysical techniques such as CD, ITC and fluorescence to characterize the peptides. His work with the protected (both N- and C-termini) penetratin analog, Pen2, as well as the synthetic peptide itself can be used as a type of control when working with the new penetratin analogs.

## 1.6 Objectives of the Research

CPPs have been a focus of many studies since their discovery, approximately 30 years ago. Many articles/reports have been published regarding CPPs' role(s) in drug delivery or their ability to deliver other macromolecules across biological membranes; but little is known about their exact mechanisms or specific interactions with the lipid membranes which they penetrate. *The overall purpose of this study is to compare biophysical characteristics of linear and cyclic CPPs by focusing on two of the first CPPs to be discovered, analogs of the peptide penetratin and of the Tat peptide.* A better understanding of these peptides' characteristics will contribute to the understanding of how different CPPs cross biological membranes.

In this study, the *first objective* was to synthesize and purify the target peptides. Solid phase peptide synthesis with Fmoc chemistry was used to synthesize the peptides followed by on-resin cyclization methods for the cyclic analogs. Reversed-phase high performance liquid chromatography was used to purify the peptides and their masses were verified by mass spectrometry.

The *second objective* was to monitor the interaction between the peptides and the lipids in the biological membranes. The peptides' secondary structures were observed to see if there is any conformational change induced by their environment. Circular dichroism and fluorescence spectroscopy were used to observe these changes. Potential peptide aggregation was monitored by comparing the overall order of the membrane lipids in the absence and the presence of the peptide. Additionally, calorimetric heat profiles were used in an attempt to determine the affinity of the peptide-lipid interactions.

## Chapter 2: Materials and Methods

The analogs of the Tat peptide and penetratin were synthesized by solid phase peptide synthesis (SPPS) using Fmoc chemistry. Two types of lipid systems were prepared as large unilamellar vesicles (LUVS), using a POPC/POPG (7:3) lipid system and a POPE/POPG (7:3) lipid system. The POPC/POPG system was used to model the membranes of negatively charged mammalian membranes and the POPE/POPG system was used to model the membranes of negatively charged bacterial membranes.<sup>25</sup> Circular dichroism and fluorescence emission spectra were used to study the conformational changes of the peptides in different environments (Table 2-1).<sup>31,32</sup> Isothermal titration calorimetry was used to determine the thermodynamic parameters of the interactions between the peptide analogs and the model lipid membranes.<sup>33</sup>

Dithiothreitol (DTT) was added to the different environments to act as a reducing agent, breaking apart and preventing disulfide bonds from occurring within the peptides and between different peptide molecules.<sup>34</sup>

**Table 2-1. Experimental methods and the corresponding biologically relevant environments.**

Environments	Fluorescence	CD	ITC
Buffer solutions	10 mM Tris-HCl, 150 mM NaCl, pH 7.4	10 mM Tris-HCl, 150 mM NaF, pH 7.4	10 mM Tris-HCl, 150 mM NaCl, pH 7.4
Organic environments	50% HFIP in buffer, 50% IsoP in buffer	50% HFIP in buffer	
Lipid systems	POPC/POPG (7:3) vesicles, POPE/POPG (7:3) vesicles	POPC/POPG (7:3) vesicles, POPE/POPG (7:3) vesicles	POPC/POPG (7:3) vesicles, POPE/POPG (7:3) vesicles

\*10 mM DTT was present in every environment.

## 2.1 Methods and Techniques

### 2.1.1 Solid Phase Peptide Synthesis

In the early 1900s the term “peptide” was coined by Emil Fischer and Ernest Fourneau.<sup>35–</sup>  
<sup>37</sup> The pair were also credited with the first peptide synthesis experiment when they reported the synthesis of the first dipeptide, glycylglycine.<sup>35,36,38</sup> In the beginning there was only solution-phase peptide synthesis, which was very limited with the types of peptides that could be synthesized. Approximately 60 years after the invention of peptide synthesis, Bruce Merrifield introduced solid-phase peptide synthesis (SPPS) to the world.<sup>36,38,39</sup> Merrifield proposed the use of a solid support made of polystyrene for peptide synthesis, a system where N<sup>α</sup>-protected amino acids could be assembled stepwise from the C terminus to the N terminus.<sup>36,39</sup> Less than a decade later, in 1970, Louis Carpino and Grace Han introduced the 9-fluorenylmethoxycarbonyl (Fmoc) N<sup>α</sup>-protecting group.<sup>36,40,41</sup> Prior to the use of the Fmoc, the protecting groups that were used required acid for removal; the Fmoc group is removed by moderate bases which ultimately provided a chemically mild alternative.<sup>36,41</sup>

Fmoc-SPPS was used to synthesize the CPPs and their analogs in this study. An advantage of using SPPS over solution-based synthesis is that soluble reagents are easily separated from the intermediate peptide chain via washing and filtration as the peptide chain is attached to the resin; this also means that excess reagents can be used to ensure the reaction goes to completion.<sup>42</sup> In SPPS, amino acids are added individually to a resin containing a solid support starting with the C-terminal amino acid and ending with the N-terminal amino acid. The Fmoc method of SPPS is a synthesis technique in which the N-termini of the amino acids are protected by a fluorenyl methoxy carbonyl (Fmoc) group. The synthesis process is a repetitive cycle of deprotection of the N-terminal group attached to the solid support (removing the Fmoc protecting group), activating the

carboxy group of the next amino acid to be added, then coupling. The basic cycle is shown in Figure 2-1. Fmoc is a base labile group that is easily altered by weak bases, thus piperidine (a mild base) is used to cleave the Fmoc group and deprotect the N-terminus. The side chain protecting groups used are not sensitive to piperidine so there is a low probability of unwanted side products forming.

N,N'-Dimethylformamide (DMF) and N-methylpyrrolidone (NMP) are two of the most common solvents used in SPSS.<sup>36,37,43,44</sup> NMP is the solvent that was used in this project as DMF has a tendency to release reactive amines which can interact with and remove the Fmoc group of the protected amino acids.<sup>37</sup> The coupling agents used in this project were 1-hydroxybenzo-triazole (HOBt) and 1H-benzotriazolium 1-[bis(dimethylamino) methylene]-5-chloro-hexa-fluorophosphate (1-), 3-oxide (HCTU).<sup>43,45</sup> HCTU is an efficient, low-cost alternative to other coupling agents; its quick coupling times also reduce the possibility of slower side reactions taking place.<sup>42,43,45</sup> Using HOBt may be redundant as HCTU is based in the triazole structure of HOBt; however, excess HOBt has been found to limit racemization.<sup>42</sup> N,N-Diisopropylethylamine (DIPEA) is added to the amino acid that is being added to the resin/peptide chain slightly before the coupling stage.<sup>42</sup> DIPEA is a mild tertiary amine base that is used to help with the activation and coupling reactions. Trifluoroacetic acid (TFA) is used to cleave the peptide from the resin and to, simultaneously, cleave protection groups from the amino acid side chains. Scavengers, such as 1,2-ethanedithiol (EDT) and triisopropylsilane (TIS), are included in the cleavage cocktail. EDT is used as a scavenger for t-butyl cations and to prevent acid catalyzed oxidation of tryptophan residues.<sup>43</sup> TIS is to quench highly stabilized cations released from cleavage of Trt blocking groups and the Rink Amide linker.<sup>43</sup>

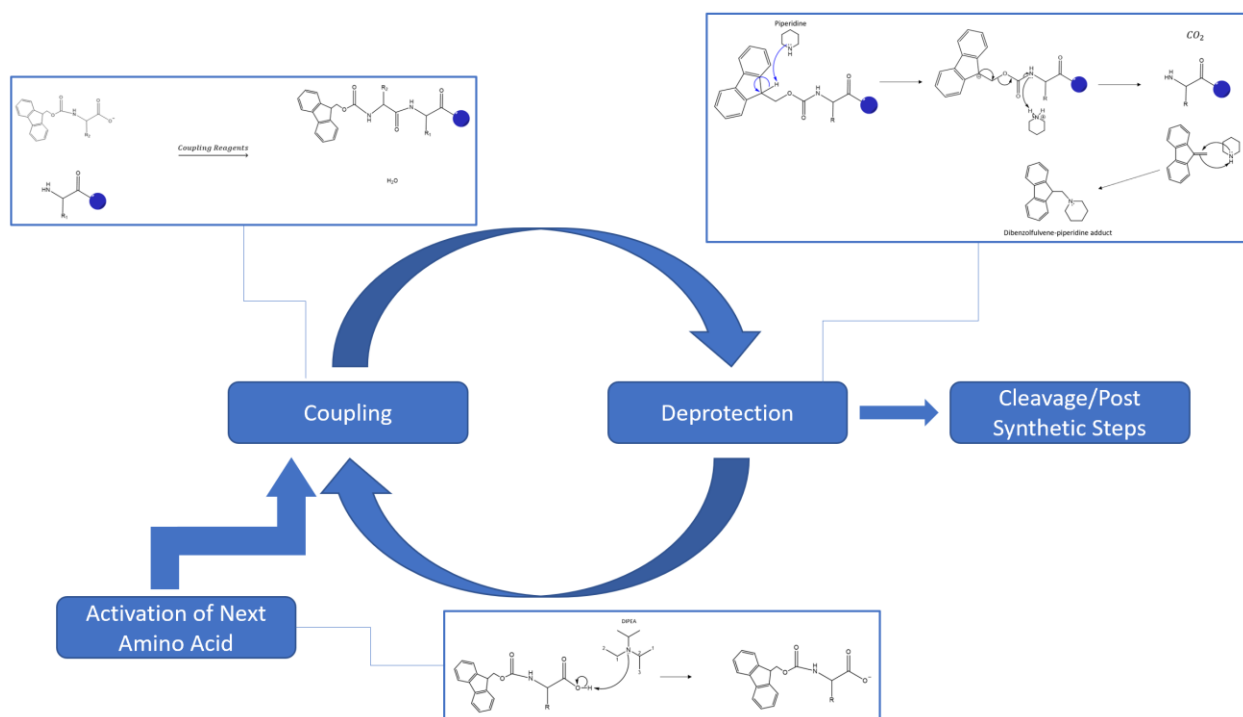


**Figure 2-1. A basic overview of Fmoc based solid-phase peptide synthesis (SPSS).**

Fmoc based SPSS is a series of repeating coupling and deprotection steps. The Fmoc group is removed from the resin/peptide chain by the addition of a mild base (piperidine). Prior to coupling the amino acid to the resin/peptide sequence, they must be activated. Activation occurs when a mild tertiary amine base (DIPEA) is added to the amino acid moments before the amino acid solution is transferred to the main reaction solution. The coupling step is where the activated amino acid is connected to the peptide chain through peptide bond formation. Coupling reagents are used to ensure efficient coupling and to reduce racemization from occurring. This figure was created using ChemDraw and Microsoft PowerPoint.

There are some amino acids or amino acid sequences that can be problematic when working with SPSS. Arginine residues can be difficult to couple to the peptide sequence due to the bulky combination of its side chain and corresponding protecting group.<sup>37,42,46</sup> Multiple, identical amino acid residues in a row in a peptide sequence can also prove challenging to synthesize.<sup>37</sup> A solution to both of these potentially problematic scenarios is to perform double coupling of the challenging amino acids.<sup>46</sup> Double coupling, as the name suggests, is performing the coupling protocol two times for a single amino acid in the sequence.<sup>46</sup> These coupling steps are done in sequence without

the normal deprotection step in between. This allows for a greater coupling efficiency, which in turn reduces the chance of deletion sequences in the crude product.<sup>37,46</sup>

### 2.1.2 Peptide Cyclization

There are two main types of peptide cyclization when it comes to cyclization after peptide synthesis; cyclization of the peptides after they have been cleaved from the resin and cyclization when the peptides are still attached to the resin. Peptides are often cyclized by the formation of a disulfide bond; studies have shown that the disulfide bond can stabilize a peptide's secondary structure which can increase pharmaceutical and biological activities of the peptide.<sup>34,47</sup> Cleavage via air oxidation is one of the most common methods of cyclization after the peptides have been cleaved from the resin. Some limitations researchers face when using this method include slow reaction rates, over-oxidation of the thiol group, low oxidation yield, and unwanted oligomerization.<sup>34,47</sup> Methods used to achieve on-resin disulfide bond formation are limited, but aim to overcome the limitations faced by air oxidation and other post-cleavage cyclization techniques.<sup>6</sup>

In 2004, Tung and his group proposed a method of on-resin disulfide bond formation in peptides utilizing different but unique cysteine protecting groups and a series of nucleophilic attacks.<sup>6</sup> An overview of the reaction is displayed in Figure 2-2. The two Fmoc-compatible thiol protecting groups used to protect the cysteine residues were the 4-methoxytrityl (Mmt) group on the polymer-bound cysteine and the tert-butylthio (S-t-Bu) group on the N-terminal cysteine. The first step of their proposed method involved the removal of the S-t-Bu group from the N-terminal cysteine by the addition of mercaptoethanol which results in a reduction reaction. 2,2'-dithiobis(5-nitropyridine) (DTNP) was then added in excess. The newly freed thiol group on the N-terminal

cysteine undergoes a nucleophilic attack on the activated disulfide of DTNP, resulting in the reprotection of the cysteine.<sup>6,48</sup> The second nucleophilic attack occurs when the peptide-resin mixture is treated with 1% TFA in DCM with TIS acting as the scavenger.<sup>6,49</sup> The mild acid conditions lead to the removal of the Mmt group from the polymer-bound cysteine. The activated free thiol of the polymer-bound cysteine then attacks that of the N-terminal cysteine causing the formation of the disulfide bond. 5-nitropyridine-2-thione is a byproduct of the cyclization reaction, which absorbs light at 386 nm. This allowed for the reaction to be monitored by measuring the absorption of the reaction.<sup>6</sup>

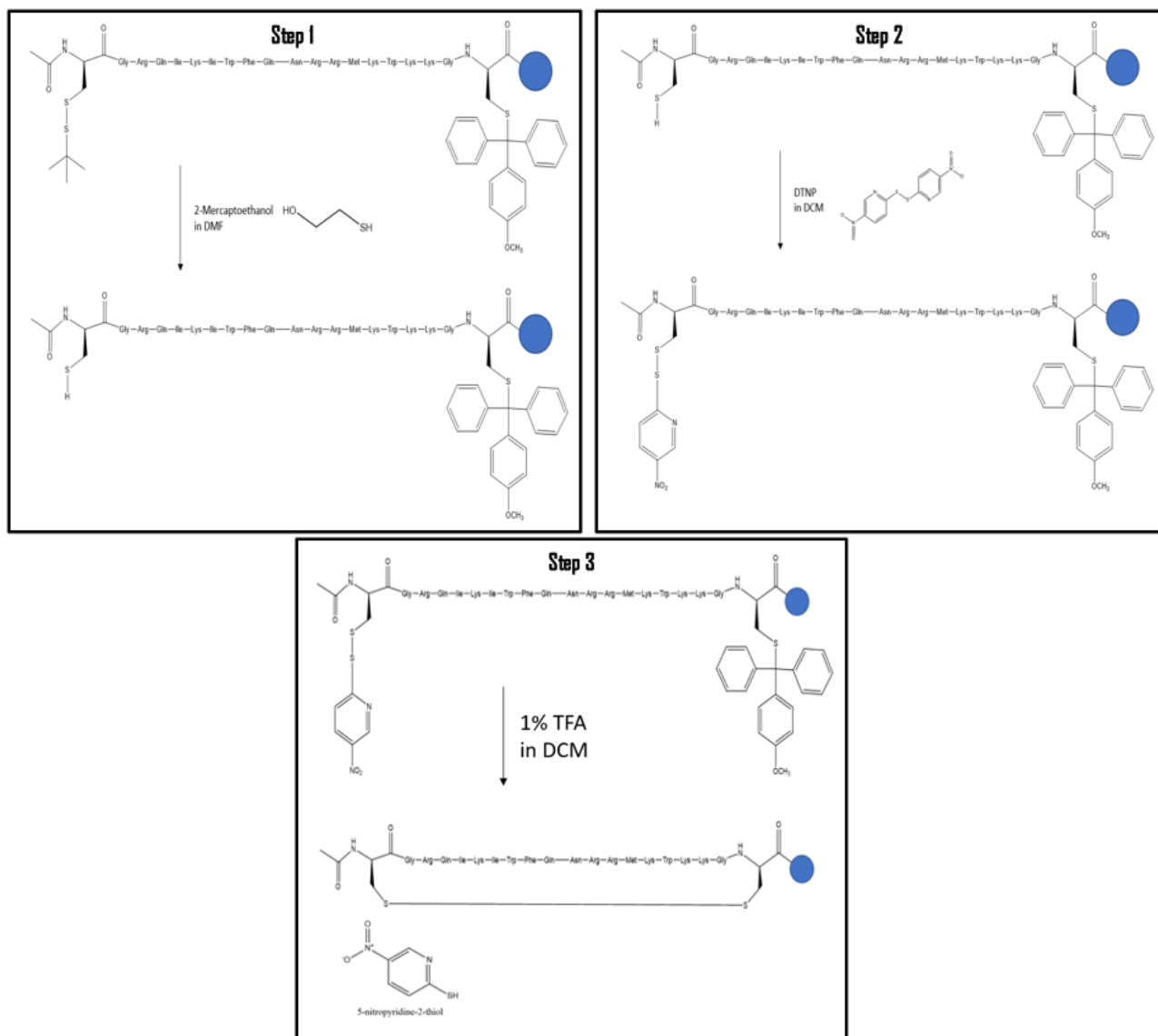


**Figure 2-2. The stepwise process of on-resin cyclization via disulfide bond formation.**

The first panel displays step 1 of the cyclization process. 2-mercaptoethanol in DMF is added to the peptide to reduce the S-S bond between the S-t-Bu group and the N-terminal cysteine, deprotecting the cysteine side chain. The second panel displays step 2 of the cyclization process in which DTNP in DCM is added in excess. The newly freed thiol group on the N-terminal cysteine undergoes a nucleophilic attack on the activated disulfide of DTNP, reprotecting the cysteine side chain. The third panel displays step 3 of the process in which cyclization of the peptide occurs. 1% TFA in DCM is added, cleaving the mmt group protecting the side chain of the C-terminal cysteine. The free thiol group of the C-terminal cysteine undergoes a nucleophilic attack on the disulfide bond protecting the N-terminal cysteine resulting in a new disulfide bond forming. A by-product of the reaction is the 5-nitropyridine-2-thione group displayed in the bottom left of the third panel. The absorbance properties of this group can be used to monitor the cyclization reaction. This figure was created using a combination of ChemDraw and Microsoft PowerPoint and was inspired by Figure 2 of reference 6. <sup>6</sup>

### 2.1.3 Peptide Purification

#### *2.1.3.1 Reverse Phase High Performance Liquid Chromatography*

Chromatography has been used to separate compounds since the 1940s, with many major breakthroughs and different techniques employed since then. One of which was the invention of High Performance (changed from Pressure) Liquid Chromatography (HPLC) in the late 1960s.<sup>50,51</sup> HPLC is a technique used to rapidly separate, identify, and quantify different components in a mixture.<sup>50-52</sup> There are two major types of HPLC; normal phase (NP) and reversed phase (RP). As with all forms of chromatography, there is a stationary phase to which the analytes bind and a mobile phase which moves the analytes through the stationary phase. The nature of these phases are where NP-HPLC and RP-HPLC differ. NP-HPLC uses a polar stationary phase and a nonpolar mobile phase, whereas RP-HPLC uses a nonpolar stationary phase and a polar mobile phase.<sup>50,52,53</sup> For this reason, RP-HPLC was used in this project, as the analytes of interest, the peptides, are polar. In RP-HPLC the analytes are eluted from the column as the polarity of the mobile phase decreases. Columns of differing types and sizes are available for use depending on the type of analytes being separated and the purpose of separation.<sup>50-53</sup> Analytical columns require low volumes and quantities of samples to be injected. Their purpose is to determine the identity, purity and quantity of the analytes in a sample.<sup>50,51</sup> Preparative (prep) and semipreparative (semi-prep) columns require larger volumes and quantities of samples to be injected, with preparative columns being a larger scale than semipreparative columns. Both preparative and semipreparative columns are used for the same purpose, to purify the analytes of interest by separating the components of the mixture into samples containing single analytes.<sup>50,51</sup>

The mobile phase used in these experiments will start with filtered Milli-Q water with 0.05% TFA, then acetonitrile (AcCN) will gradually be added to decrease the polarity. TFA is

included in the mobile phase to enhance peptide separation. It interacts with the side chains of basic amino acid residues and can provide an acidic environment where the acidic amino acid residues are protonated which leads to increased interaction between the peptide and the stationary phase. In the current project analytical RP-HPLC was first used to analyze the purity of the synthesized crude peptide sample; then, based on the analytical data, a semi-prep column was used to separate and isolate the different components to obtain a pure peptide. A second round of analytical RP-HPLC was conducted to verify the homogeneity of the peptide that was purified using the semi-prep column. Mass spectrometry, more specifically electrospray ionization mass spectrometry (ESI-MS), was used to compare the masses in the crude and pure sample to the hypothetical mass of the peptide to ensure that the peptide of interest was correctly synthesized and purified. ESI-MS was performed by an outside service provider, Dr. Ning Zhibin, of the University of Ottawa.

#### 2.1.4 Lipid Vesicle Preparation

LUVs were used as model lipid membranes (previously described in section 1-4) and were prepared with a diameter around 100 nm using the extrusion technique.<sup>54</sup> LUVs of two different lipid compositions were prepared and used in the experiments described below. The two LUV systems contained a mixture of PC and PG, or a mixture of PE and PG. The PC:PG and PE:PG systems will mimic negatively charged mammalian and bacterial membranes, respectively.

#### 2.1.5 Circular Dichroism Spectroscopy

Circular dichroism (CD) spectroscopy was used to measure the secondary structure of the peptides in different environments. Changes in the secondary structure of the peptides due to interactions with the different environments can yield information related to the activity or mechanism of said peptide.

CD is an optical phenomenon caused by unequal absorbance of left and right-handed circularly polarized light.<sup>55</sup> When peptides (or other asymmetric molecules) come in contact with light they can absorb the left and right-handed circularly polarized light at different rates and have different indices of refraction, which results in the light being elliptically polarized.<sup>55</sup> The difference between the ellipticities can be measured in degrees of ellipticity and converted to mean residual ellipticity (MRE) by considering the peptide concentration and number of amino acids. MRE is measured  $\text{deg.cm}^2.\text{dmol}^{-1}$  and is represented by  $\theta$ .<sup>56</sup> The amide groups in the peptide backbone act as chromophores in the far-UV range of the spectra, which absorb the polarized light.<sup>57</sup> Figure 2-3 shows the spectra of common secondary structures. As can be seen in Figure 2-3, proteins and peptides containing  $\alpha$ -helical structures show minima around 208 and 222 nm and a maximum around 190 nm; containing  $\beta$ -sheets display a broad negative band with a minimum around 218 nm and a positive band with a maximum around 193 nm; containing random or unordered structure with a minimum around 197 nm and a positive, broad band with a small maximum around 217 nm.<sup>55,56,58</sup>

CD measurements of penetratin and Tat peptides were compared in buffer, 50% hexafluoro-2-propanol (HFIP), and in the two types of the aforementioned LUVs to detect environment-dependent changes in conformation. HFIP, among other fluorinated alcohols, has been used as a structure-inducing solvent for many years; it enhances the structure of small proteins in peptides which are normally unstructured in aqueous environments.<sup>10,59-63</sup> It has been suggested that molecules of HFIP associate with the hydrophobic surface of  $\alpha$ -helices and  $\beta$ -strands in a way that the alcohol mimics the interior of a lipid membrane or folded protein.<sup>60</sup> HFIP in particular is seen as one of the most effective cosolvents for stabilizing the structure of peptides that form secondary structures.<sup>62</sup>

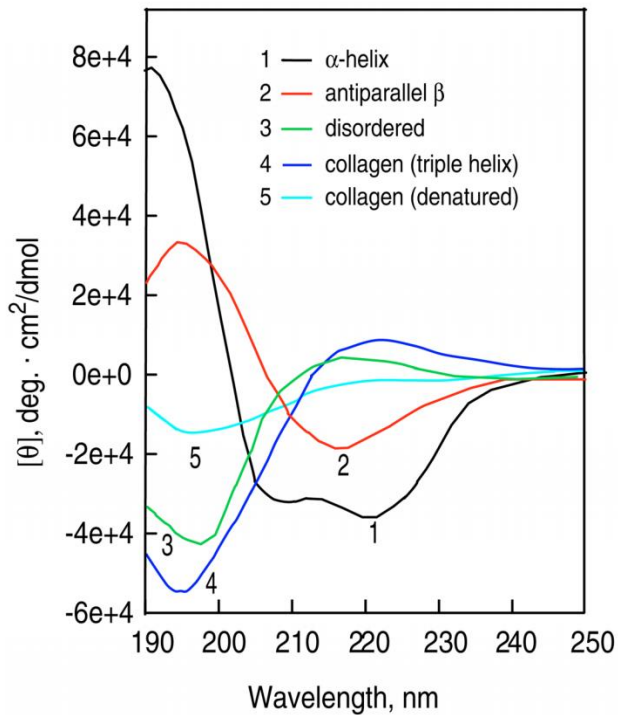


**Figure 2-3. CD spectra of protein backbone corresponding to common secondary structures.**

Circular dichroism spectra of five common secondary structures ( $\alpha$ -helical (black), antiparallel  $\beta$ -sheet (red), unordered/disordered (green), collagen forming a triple helix (dark blue), and denatured collagen (light blue) displayed in wavelength vs degrees ellipticity. This figure was taken from reference 55, with permission, where it can be seen as part of Figure 1.<sup>55</sup>

### 2.1.6 Fluorescence Spectroscopy

Fluorescence is a spectroscopic technique that has been used to study proteins since the early 1960s.<sup>32,64</sup> It is one of the most commonly used spectroscopic techniques in the worlds of biophysics and biochemistry, as it is a highly sensitive technique that is non-invasive and non-destructive.<sup>32,65</sup> Fluorescence spectroscopy is based on the emission of light by a chemical compound that has absorbed light or electromagnetic radiation at a shorter wavelength than that which was emitted.<sup>32,65,66</sup> The mechanism of fluorescence can be seen below in Figure 2-4, in the form of a Jablonski diagram. The diagram was named after and introduced by Alexander Jablonski

who was best known as the father of fluorescence spectroscopy.<sup>32</sup> Following the absorption of light, a fluorophore is usually excited to some higher vibrational energy level ( $S_1$  or  $S_2$ ).<sup>32</sup> The light that is emitted when the electron relaxes from the  $S_1$  to the  $S_0$  energy level is what is known as fluorescence.<sup>32</sup> This emitted fluorescence light has a longer wavelength (lower energy) than that of the absorbed light as some energy is lost to non-radiative relaxation via heat formation or in some cases the intersystem crossing which leads to phosphorescence.<sup>32</sup>

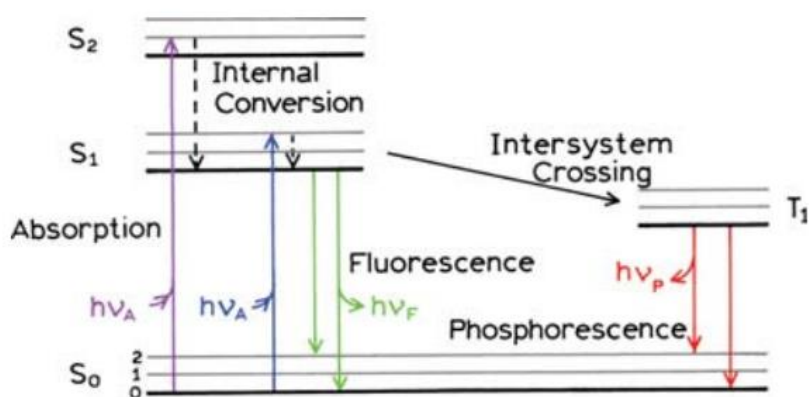


**Figure 2-4. A Jablonski diagram demonstrating the mechanism of fluorescence.**

$S$  indicates different energy states of an electron.  $S_0$  represents the ground state while  $S_1$  and  $S_2$  indicate higher energy states.  $T_1$  represents the first transition state which is not relevant to the fluorescence spectroscopy experiments. This figure is taken from Reference 32, with permission, where it can be seen as Figure 1.5.<sup>32</sup>

Like CD, fluorescence can be used to study the interaction between peptides and their environment. The three aromatic amino acids can act as fluorophores.<sup>32</sup> The three amino acids and the wavelengths at which they absorb and emit light in aqueous environments are as followed: phenylalanine residues absorb light around 260 nm and have a fluorescence emission wavelength around 282; tyrosine residues absorb light around 275 nm and have a fluorescence emission around 303 nm; tryptophan residues absorb light at a wavelength of 280 nm and have varying emission wavelengths depending on the surrounding environment.<sup>32</sup>

In this research project fluorescence emission spectra of the penetratin and Tat peptides in different environments was observed using a Cary Eclipse Fluorescence Spectrometer. Both peptides contain at least one aromatic residue, penetratin has two tryptophan residues while Tat peptide contains one tyrosine which can act as fluorophores.<sup>67</sup> The fluorescence emission spectra of the peptides can give information on the environment surrounding the fluorophore, which in turn can give information about conformational changes or interactions of the peptide with its given environment. Tryptophan fluorescence is very sensitive to its environment, but tyrosine fluorescence is relatively insensitive.<sup>67</sup> Tyrosine fluorescence emission spectra are still used in measuring protein fluorescence as they can indicate slight conformational changes at the surface which tryptophan residues buried in the hydrophobic core could not.<sup>68</sup> Structural rearrangements can lead to the enhancement of the tyrosine fluorescence, if the tyrosine is separated from a group causing the quenching.<sup>68</sup> In most protein-related cases, tyrosine fluorescence is either quenched by excitation energy transfer to tryptophan or ionization of the residue by neighbouring carboxyl or amino groups.<sup>68</sup> The emission spectra of tryptophan can shift left or right depending on its environment with a  $\lambda_{\text{max}}$  ranging from 308-355 nm.<sup>67</sup> Lower wavelengths indicating that the tryptophan is in a more hydrophobic (less polar) environment, also known as a blue shift. A red shift occurs when the tryptophan fluorescence shifts to a higher wavelength indicating a less hydrophobic (more polar) environment.<sup>67</sup>

A shift in the emission spectra is one change that can be seen as a result of the fluorophore interacting with different environments, a second change leads to a decrease in the fluorescence intensity of the sample.<sup>32</sup> This change is a result of fluorescence quenching. Quenching can be caused by a number of molecular interactions, including but not limited to: molecular rearrangements, energy transfer, ground-state complex formation, collisional/dynamic quenching

and excited-state reactions.<sup>32</sup> There are many substances that can act as quenchers of tryptophan fluorescence emission through the interactions listed above, including amino acids and reagents used in this research project.<sup>64,67</sup> Main chain amides and the sidechains of certain amino acids, such as cysteine and histidine, quench tryptophan fluorescence by excited-state electron transfer.<sup>64</sup> Amino acid side chains, such as that of lysine, quench tryptophan fluorescence by excited-state proton transfer.<sup>64</sup>

### 2.1.7 Isothermal Titration Calorimetry

Isothermal titration calorimetry (ITC) is used to observe interactions between molecules and their surrounding environment if there is a release or absorbance of energy in the form of heat (or enthalpy) of interaction by the system.<sup>33,69,70</sup> The technique was invented in 1988 and has been a popular technique for determining thermodynamic parameters of interactions since.<sup>33</sup> The enthalpy ( $\Delta H$ ), entropy ( $\Delta S$ ), binding free energy ( $\Delta G$ ), association constant ( $K_a$ ), reaction stoichiometry ( $n$ ), and the heat capacity ( $\Delta C_p$ ) of the reaction can all be determined using ITC.<sup>71</sup> An example of such an interaction is a peptide or protein interacting with a model membrane like lipid vesicles.<sup>70,72</sup>

The ITC instrument is made up of two cells; the reference cell, which holds the solvent and the sample cell, which is where the titration takes place.<sup>33</sup> Both cells are kept at steady pressure and temperature throughout the experiment.<sup>33</sup> The ligand is slowly titrated into the sample cell via a syringe and the heat released or absorbed due to the interaction of the ligand and target molecule will temporarily change the temperature within the sample cell.<sup>33</sup> The instrument not only detects this change in temperature but it also brings the temperature of the sample cell back to its original temperature, in line with that of the reference cell.<sup>33,70</sup> The amount of power required to maintain

the temperature is used to calculate the heat change, this is done by integrating the power over the time resulting in the enthalpy of the reaction.<sup>33</sup> The amount of heat released or absorbed throughout the experiment corresponds to the fraction of bound ligand, as the substrate will become more saturated as the ligand concentration continues to increase with each injection.<sup>33</sup>

## 2.2 Materials and Experimental Procedures

### 2.2.1 Solid Phase Peptide Synthesis

#### 2.2.1.1 Materials

All peptides were synthesized by solid-phase Fmoc chemistry procedures on Fmoc-protected Rink resin (Matrix, Quebec, Canada). Fmoc-protected amino acids used for peptide synthesis were purchased from either Novabiochem, EMD Biosciences or Advanced Chemtech. DCM (Sigma Aldrich, Milwaukee, USA) and NMP (EMD chemicals Inc. Darmstadt, Germany) were used as solvents. HCTU (Matrix, Quebec, Canada), HOBt (Advanced Chemtech, Louisville, Kentucky, USA), and DIPEA (Matrix, Quebec, Canada) were used in the coupling stage. Piperidine (EMD chemicals Inc. Darmstadt, Germany) was used in the deprotection stage. DTNP (Sigma Aldrich, Milwaukee, USA) and  $\beta$ -mercaptoethanol (Sigma Aldrich, Milwaukee, USA) were used in peptide cyclization. The cleavage cocktail contained 94% TFA (Sigma Aldrich, Milwaukee, USA), 2.5% water (filtered, Milli-Q), 2.5% EDT (Sigma Aldrich, Milwaukee, USA), and 1% TIS (Sigma Aldrich, Milwaukee, USA). Diethyl ether (Sigma Aldrich, Milwaukee, USA) was used to precipitate the peptide.

#### 2.2.1.2 Experimental Procedures

*Protected Peptide Synthesis.* 0.05 mmol of Rink resin ( $0.53 \text{ mmol} \cdot \text{g}^{-1}$ ) was transferred to a reaction vessel to start the synthesis. The resin was swollen in DCM for 20 minutes, then DCM

was removed via vacuum filtration. The resin was further swollen in NMP for 20 minutes. The NMP was removed via vacuum filtration, then the Fmoc group was removed through the deprotection process; the addition of 20% piperidine in NMP added to the swelled resin and shook for 25 minutes. The excess solution with the deprotected Fmoc were removed via vacuum filtration and the deprotected resin was rinsed 5 times with NMP. The next amino acid was activated simultaneously, as the deprotection was taking place. To activate the next amino acid, 0.25 mmol of the amino acid, 0.25 mmol HOBt and 0.25 mmol HCTU were dissolved in NMP on a mechanical stirring plate for 15-20 minutes, then 30-45 seconds before the amino acid mixture was added to the reaction vessel, 0.5 mmol of DIPEA was added to the amino acid mixture. The activated amino acid mixture was then transferred to the reaction vessel, a steady stream of nitrogen gas was used to remove any oxygen from the reaction vessel. This mixture was then left to shake for 45-55 minutes; this step was known as the coupling step. The deprotection and coupling steps were repeated until all amino acids in the peptide sequence had been coupled and all Fmoc groups had been removed. Once the final amino acid had been added and deprotected, the N-terminus of the peptide was then protected via acetylation. N-terminal acetylation was achieved by adding 2.5 mmol of DIPEA and 2.5 mmol acetic anhydride in NMP and transferring this mixture to the reaction vessel and shaking for 30 minutes. Excess acetylation reagents were removed by rinsing with NMP under vacuum filtration. The peptide-resin mixture was rinsed with DCM and dried under vacuum filtration and placed in a vacuum desiccator overnight. Then either peptide-resin cleavage or peptide cyclization was performed.

Peptide Cyclization. The peptides which were intended to be cyclized were synthesized using the above procedure. The only deviation to the above procedure was that cysteines with specific side chain protecting groups were used, the N-terminal cysteine had a s-t-Bu protecting

group and the C-terminal cysteine had a mmt protecting group. The dried peptide-resin mixture was swollen in DCM for 20 minutes and then NMP for 20 minutes, following the same steps as the swelling in peptide synthesis.  $\beta$ -mercaptoethanol (20%) in NMP was added to the reaction vessel with the swelled peptide-resin mixture and left to shake for 3 hours to remove the stub group from the N-terminal cysteine. Simultaneously, 0.5 mmol DTNP was dissolved in 3 mL DCM via stir bar and mechanical stir plate. After the 3 hours had passed, the reaction vessel was rinsed thoroughly with NMP followed by DCM. Then the DTNP in DCM was transferred to the reaction vessel and left to shake for 1 hour to reprotect the N-terminal cysteine and activate the 5-Npys protecting group. The reaction vessel was then rinsed thoroughly with DCM, until the filtrate is no longer orange. TFA (1%) in DCM with 2% TIS included as a scavenger was then transferred to the reaction vessel to complete the cyclization step. The cyclization reaction was monitored by taking UV absorption measurements of the solution at 386 nm every 15-20 minutes. The peptide-resin mixture was then rinsed with DCM and dried under vacuum filtration before being placed in a vacuum desiccator to dry overnight. Peptide-resin cleavage was then performed.

Peptide-resin Cleavage. The peptides were cleaved from Fmoc-Wang resin using a cleavage cocktail solution. The components of the cleavage cocktail were determined using Figure 2-5 based on the amino acid composition and their corresponding side chain protecting groups. The cleavage cocktail used for each peptide contained 94% TFA, 2.5% ultrapure H<sub>2</sub>O, 2.5% EDT and 1% TIS. The cocktail solution (3 mL) was transferred to the dried peptide-resin mixture in the reaction vessel. A light, steady stream of nitrogen gas was applied to the mixture to remove any oxygen from the vessel. The mixture was then shaken for 2 hours, then another 1.5 mL of the cocktail was added to the mixture and the procedure was repeated; this was done once more for a total addition of 6 mL cleavage cocktail being added and 6 hours of shaking. The reaction vessel

was then clamped to a retort stand with a pre-weighted round bottom flask clamped directly below. The peptide solution was then allowed to drain from the reaction vessel into the round bottom flask. The reaction vessel was rinsed with approximately 1 mL of the cleavage cocktail four times, for a total of 4 mL cocktail used for rinsing; nitrogen gas was applied to the top of the reaction vessel to allow for a more efficient transfer of peptide solution to the round bottom flask. The cocktail solution was then evaporated in the fume hood by applying a stream of steady nitrogen gas, light enough to slightly disturb the surface of the solution without splashing, while rotating the flask resulting in a thin peptide film around the bottom half of the round bottom flask. Cold diethyl ether was then used to rinse and precipitate the peptide out of any remaining solution. The diethyl ether was removed via Pasteur pipettes, carefully to ensure minimal amount of crude peptide was lost. The round bottom flask with the peptide was then dried in a vacuum desiccator overnight prior to weighing and further use.

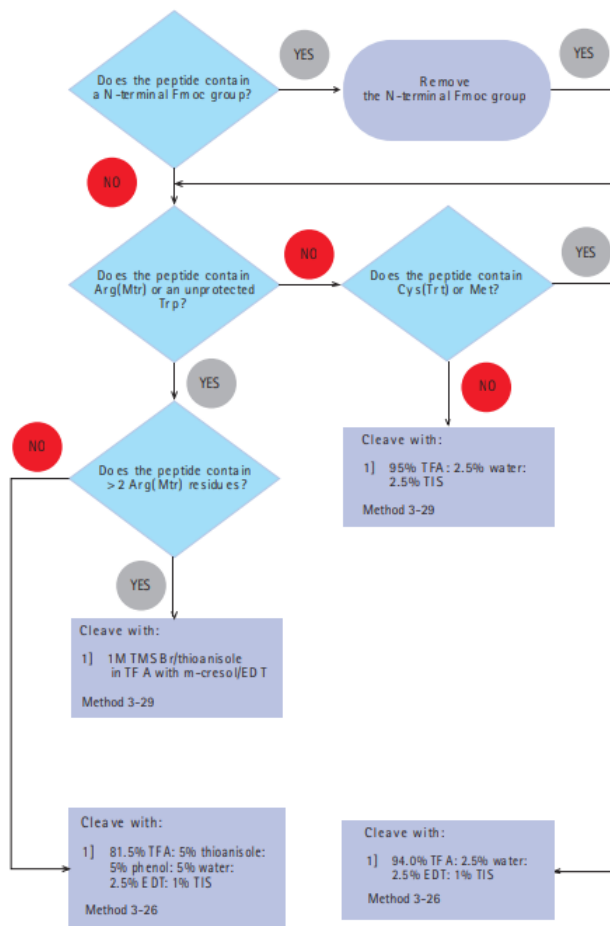


**Figure 2-5. Flow-chart for selecting the appropriate cleavage cocktail for Fmoc SPPS based on peptide sequence.**

The systematic steps used to determine the optimal recipe for the cleavage cocktail based on the sequence of the target peptide is displayed. This figure was taken from reference 43 where it can be seen as Figure 3-33.<sup>43</sup>

## 2.2.2 Peptide Purification

### 2.2.2.1 Reverse Phase High Performance Liquid Chromatography

#### 2.2.2.1.1 Materials

Synthetic peptides, TFA (Sigma Aldrich, Milwaukee, USA), acetonitrile (filtered, HPLC grade, EMD chemicals Inc. Darmstadt, Germany), methanol (filtered, HPLC grade, Sigma Aldrich, Milwaukee, USA), water (filtered, Milli-Q).

#### 2.2.2.1.2 Experimental Procedures

Analytical HPLC. Luna® Omega 5 µm Polar C18 100 Å (4.6 mm x 250 mm) was used as a stationary phase. Approximately 1 mg of peptide was dissolved in 100 µL filtered Milli-Q water. The peptide solution was further dissolved in a bath-sonicator, 5 minutes under the degas setting. The autoinjector system injected 15 µL of the dissolved and degassed solution into the column at a time.. The mobile phase was eluted over a linear gradient from 100% water (with 0.05% TFA) to 100% acetonitrile (with 0.05% TFA) over 30 minutes with a flowrate of 0.75 mL/min. The mobile phase, consisting of 100% acetonitrile (with 0.05% TFA) was then eluted for an extra 5 minutes with a flowrate of 0.75 mL/min to ensure all compounds had eluted from the column.

Semi-preparative HPLC. Luna® Omega 5 µm Polar C18 100 Å (10 mm x 250 mm) was used as a stationary phase. Approximately 10 mg of crude peptide was dissolved in 2.5 mL filtered Milli-Q water. The peptide solution was further dissolved in a bath-sonicator, 5 minutes under the degas setting. The dissolved and degassed solution was injected into the HPLC system. The mobile phase was eluted over a linear gradient from 100% water (with 0.05% TFA) to 100% acetonitrile (with 0.05% TFA) over 30 minutes with a flowrate of 3.00 mL/min. The samples were collected in vials every 10 seconds (0.5 mL collections) when a peak appeared on the chromatogram at the corresponding wavelengths (220 nm for all peptides, 275 nm for peptides containing tyrosine residues, and 280 nm for peptides containing tryptophan residues). The mobile phase, consisting of 100% acetonitrile (with 0.05% TFA) was then eluted for an extra 5 minutes with a flowrate of 3.00 mL/min to ensure all compounds had eluted from the column. This process was repeated until the crude peptide had been passed through the HPLC column.

### 2.2.2.2 Pure Peptide Preparation and Estimation

#### 2.2.2.2.1 Materials

Synthetic peptides, liquid nitrogen, water (filtered Milli-Q).

#### 2.2.2.2.2 Experimental Procedures

Rotary Evaporation Under Vacuum: The collected sample fractions that corresponded to the same peaks were pooled together in pre-weighted round bottom flasks. The round bottom flasks were then connected to the rotary evaporator system one at a time and lowered into the 37° C water bath. Vacuum was applied to the system and the sample was slowly rotated to remove any organic solvent (acetonitrile and TFA) from the pooled fractions. Liquid nitrogen was used to condense the evaporated materials in a trap once they begin to evaporate. The round bottom flasks were then removed and cooled to room temperature.

Lyophilization: The mouth of the round bottom flasks containing the pooled peptide fractions were covered with kimwipes and flash frozen in liquid nitrogen. The frozen samples were then lyophilized resulting in peptides in their solid state (powder) form.

Verification of Peptide's Mass: The purity of the fractions was verified using analytical HPLC following the experimental procedure listed above. The peptide sequences were then verified by ESI-Mass Spectroscopy at the University of Ottawa by Dr. Ning Zhibin (Table 3-1). The relative concentration of the peptide samples was then determined by measuring their UV absorbance at 280 nm and applying Beer's Law. The molar extinction coefficient values were calculated using *The Edelhoch Method*, based on the number of tryptophan, tyrosine and cystine residues in their expected sequences.<sup>73</sup>

### 2.2.3 Lipid Vesicle Preparation

#### *2.2.3.1 Materials*

Lipid stock solutions in chloroform in a 7:3 ratio (POPC:POPG, POPE:POPG). The lipids (Avanti Polar Lipids, Alabama) used to create the stock solution were as follows: 1-palmitoyl-2-oleoyl-sn-3-glycero-phosphatidylcholine (POPC), 1-palmitoyl-2-oleoyl-sn-3-glycero-phosphatidylglycerol (POPG), 1-palmitoyl-2-oleoyl-sn-3-glycero-phosphatidylethanolamine (POPE). Buffer solution (Table 2-1), DTT (BioShop Canada), water (filtered Milli-Q).

#### *2.2.3.2 Experimental Procedures*

25 mg/mL POPC, POPE and POPG stocks in chloroform were transferred to round bottom flasks to create the 7:3 molar ratios of POPC:POPG and POPE:POPG. A light but steady stream of nitrogen gas was applied to the round bottom flasks while rotating the flasks to evaporate the chloroform and leave a thin lipid film around the bottom half of the round bottom flask. The lipid film was then placed in a vacuum desiccator overnight to further dry. The lipid film was rehydrated by transferring a proportional amount of buffer and then vortexed to ensure the film was completely hydrated and detached from the glass. The lipids were then freeze thawed by flash freezing in liquid nitrogen and then thawed in a water bath set to approximately 30 °C. This freeze thawing process was repeated 2 times for a total of 3 freeze thawing cycles. LUVs were then formed by extruding the freeze thawed lipid solution through a 100 nm filter in a mini extruder (Avanti Polar Lipids, Alabama).

### 2.2.4 Circular Dichroism Spectroscopy

#### *2.2.4.1 Materials*

Synthetic peptides, lipid vesicles (PC/PG, PE/PG), CD buffer solution (Table 2-1), DTT (BioShop Canada), HFIP, water (filtered Milli-Q).

#### *2.2.4.2 Experimental Procedures*

Far-UV CD spectra of the peptides were measured by an Aviv 215 spectropolarimeter (Aviv Biomedical, NJ) in the presence of buffer and the combination of buffer and other organic environments. The CD buffering solution contained 10 mM Tris-HCl and 150 mM NaF at pH 7.4. The CD samples were prepared in a 1.5 mL microcentrifuge tube. The sample components (peptide, 4x CD buffer, DTT and water) were individually added to the microcentrifuge tube with the organic environment component (either alcohol or liposome mixture) being added last. The mixture was aspirated using a micropipette 10 times immediately after the addition of the alcohol or liposome component. Approximately 350  $\mu$ L of the sample mixture was transferred to a high precision quartz cuvette with a 1 mm path length and placed inside the spectropolarimeter. The spectra were measured in the far-UV range between 260 nm and 195 nm, the ellipticities were then converted to mean residue ellipticity.

#### 2.2.5 Fluorescence Spectroscopy

##### *2.2.5.1 Materials*

Synthetic peptides, L-tryptophan (Sigma-Aldrich), lipid vesicles (PC/PG, PE/PG), fluorescence buffer solution (Table 2-1), CD buffer solution (Table 2-1), DTT, alcohol (HFIP, isopropanol), water (filtered Milli-Q).

##### *2.2.5.2 Experimental Procedures*

Fluorescence emission spectra of the peptides in different environments was measured using a Cary Eclipse Fluorescence Spectrometer (Agilent, California) in the presence of buffer and the combination of buffer and other organic environments. The fluorescence buffering solution contained 10 mM Tris-HCl and 150 mM NaCl at pH 7.4. The samples were prepared using the

same procedural steps as the Circular Dichroism samples listed above. Approximately 650  $\mu\text{L}$  of the sample mixture was transferred to a high precision quartz cuvette with a 1 cm path length and placed inside the spectrometer. The tryptophan containing samples (Penetratin analogs) were excited at 280 nm and the tyrosine containing samples (tat analogs) were excited at 275 nm. Emission data was collected from 290-500 nm at 280 nm excitation wavelength and 285-500 nm at 275 nm excitation wavelength.

## 2.2.6 Isothermal Titration Calorimetry

### *2.2.6.1 Materials*

Synthetic peptides, lipid vesicles (PC/PG, PE/PG), ITC buffer solution (Table 2-1), water (filtered Milli-Q).

### *2.2.6.2 Experimental Procedures*

A VP-ITC microcalorimeter (MicroCal, NJ) was used to conduct the ITC measurements. 2.5 mL peptide samples in buffer (or just buffer for the blank) were prepared for each measurement. 300  $\mu\text{L}$  of liposome solution was also used for each measurement. Two LUV systems were used for ITC experiments: POPC:POPG and POPE:POPG, both in 7:3 molar ratios. The lipid vesicles were rehydrated in 10 mM Tris and 150 mM NaCl buffer at pH 7.4 to maintain an identical buffer composition inside the liposomes as was outside the liposomes during the measurements. The peptide-buffer and blank buffer samples, and LUV solutions were degassed under reduced pressure for 5 minutes, with the peptide samples being stirred simultaneously via magnetic stir bar. The reference cell of the VP-ITC instrument was filled with degassed water prior to use; the same reference was used for all experiments. 2-2.5 mL of the degassed peptide or blank samples were brought up into a Hamilton syringe and injected into the sample cell until the cell

begins to overflow. The sample cell volume is 1.4352 mL. The degassed LUV samples were brought up into the ITC syringe and were purged 2 times by the software to remove any gas. The syringe containing the LUVs was then carefully inserted into the sample cell with the blank or peptide solution. The ITC measurement conditions can be seen below in Table 2-2. Heat flow per injection was then measured and later corrected by subtracting the blank from the measurements with peptide solution.

**Table 2-2. Isothermal Titration Calorimetry measurement conditions.**

Total number of injections	30
Cell temperature (°C)	30
Reference power (µcal/sec)	15
Initial delay (s)	60
Stirring speed (rpm)	300
Volume (µL)	10
Duration (s)	20
Spacing (s)	180
Filter Period (s)	2

## **Chapter 3: Results and Discussion**

### **3.1 Synthesis and Purification of the Cell-Penetrating Peptides**

Four CPPs, two analogs of the penetratin peptide and two analogs of the Tat peptide, were synthesized by SPPS using Fmoc-chemistry. Each analog pairing shared the same amino acid sequence, the difference in the analogs was that one of each pair was linear while the second member of each pair was cyclic. Each of the four analogs were synthesized in a way that both their N- and C-termini were protected by acetyl and amide groups, respectively. The decision to protect

the termini was made as the peptides are found as part of larger proteins in nature, therefore their termini would in a sense be protected by the amino acids on either side of the peptide sequence. One other modification was done to each of the peptides' native sequence. One glycine and cysteine residue were added to both the N and C-termini of each peptide (the cysteine residues were the terminal residues which were protected by the acetyl and amide groups). These modifications were made to facilitate the cyclization of the peptides through disulfide bond formation through the thiol groups of the cysteines, with the glycine residues adding additional flexibility to enhance the likelihood of a successful cyclization reaction. As mentioned previously, the native sequence of the Tat peptide is YGRKKRRQRRR and the native sequence of the penetratin peptide is RQIKIWFQNRRMKWKK. Therefore, the sequences of the protected Tat and penetratin analogs synthesized with the modifications described for the current study were Ac-CGYGRKKRRQRRRGC-amide and Ac-CGRQIKIWFQNRRMKWKKGC-amide, respectively, where Ac represents an acetyl group. The protected Tat analogs were labelled pTatL and pTatC, where "p" indicates that the termini are protected, "L" indicates a linear peptide, and "C" indicates a cyclic peptide. The penetratin analogs were labelled pPenL and pPenC following the same notation style.

Penetratin and the Tat peptide were the CPPs chosen for this research due to their similarities and the extensive studies that had been conducted on the two peptides. At pH 7.4, which the experiments in this project took place, the penetratin analogs had a net charge of 6.8 and the Tat peptide analogs had a net charge of 7.8. Both peptides are rich in arginine and lysine residues which contribute to their polar natures.<sup>13,18</sup> The Tat peptide analogs contain one tyrosine residue which was used to monitor absorbance (RP-HPLC) and fluorescence.<sup>13</sup> The penetratin analogs contain two tryptophan residues, W8 and W16.<sup>18</sup> Unlike the Tat peptide analogs, the

penetratin analogs contain a phenylalanine residue, which contains a nonpolar side chain and can also be used to measure absorbance and fluorescence (often impractical due to weak intensity).<sup>18</sup> In lipid membrane models, the two tryptophan residues in the penetratin analog can possess different fluorescence properties in different environments (with different polarities), which can be manipulated to determine their relative location in lipid membrane models.

All four peptides were synthesized, with the cyclic analogs generated using the process described in Chapter 2. However, only the linear analogs were successfully purified via RP-HPLC. This was believed to be due to incomplete cyclization of the peptides. The Tat analogs, although short in sequence, were challenging to synthesize due to their specific amino acid sequence. As mentioned previously, arginine residues can be problematic to deal with during SPPS because of the bulky nature of their side chain and side chain protecting groups. Arginine residues also make up approximately 40% of the Tat analog's sequence. Multiple identical amino acids that occur back-to-back in a sequence can also prove troublesome, which as can be seen in the Tat analog's sequence, occurs often. Both issues were overcome using a series of double coupling steps for each potentially problematic amino acid in the Tat analog's sequence. The same was also done, for consistency, with the penetratin analog's sequence. The analytical chromatograms corresponding to the unsuccessful cyclized analogs pTatC and pPenC can be seen in the appendix as Figures A1 and A2, respectively.

Figure 3-1 displays the corresponding chromatograms for the purification of the pTatL analog via RP-HPLC. The small chromatograms in the top left (or top right in the case of chromatogram C), are the zoomed in image of the areas within the blue box in the main chromatogram. Chromatograms A and B show the results from the analytical RP-HPLC of the crude pTatL peptide, prior to any purification techniques. Figure 3-1 A is the analytical

chromatogram of pTatL detected at 220 nm and Figure 3-1 B is detected at 275 nm. Chromatograms A and B are from the same RP-HPLC experiment, with A (220 nm) indicating components of the crude mixture containing peptide bonds and B (275 nm) indicating components of the crude mixture containing tyrosine residues. In both cases, there was a major peak at a retention time of 15.81 minutes corresponding to the peptide of interest (pTatL). Smaller peaks in A and B can be seen, which indicate impurities in the sample or potential artifacts. Semipreparative RP-HPLC was performed to remove these impurities. An example of a chromatogram from the semipreparative RP-HPLC experiment done to purify the pTatL peptide is displayed in Figure 3-1 C. Chromatogram C displays the visual results of the experiment detected at 220 nm, both 220 nm and 275 nm were observed when conducting these experiments with fractions being collected for the peaks that appeared on both chromatograms at the same retention times. It was determined that the peak displayed in C that corresponded to the pTatL was the peak that eluted between 11.70 and 12.05 minutes. This was confirmed by a second round of analytical RP-HPLC which is displayed in Figure 3-1 D and E, which again show the exact same sample but detected at 220 nm and 275 nm, respectively. The complete purification of the pTatL peptide (100% purity, practically impossible) was not accomplished after one round of semipreparative RP-HPLC as can be seen by the minor peaks in chromatograms D and E. The purity of the sample was estimated to be 88% pure, this estimation was performed by the Waters HPLC software which compared the area under the major peak at 17.17 minutes to the summation of the area under the peaks in the chromatogram.

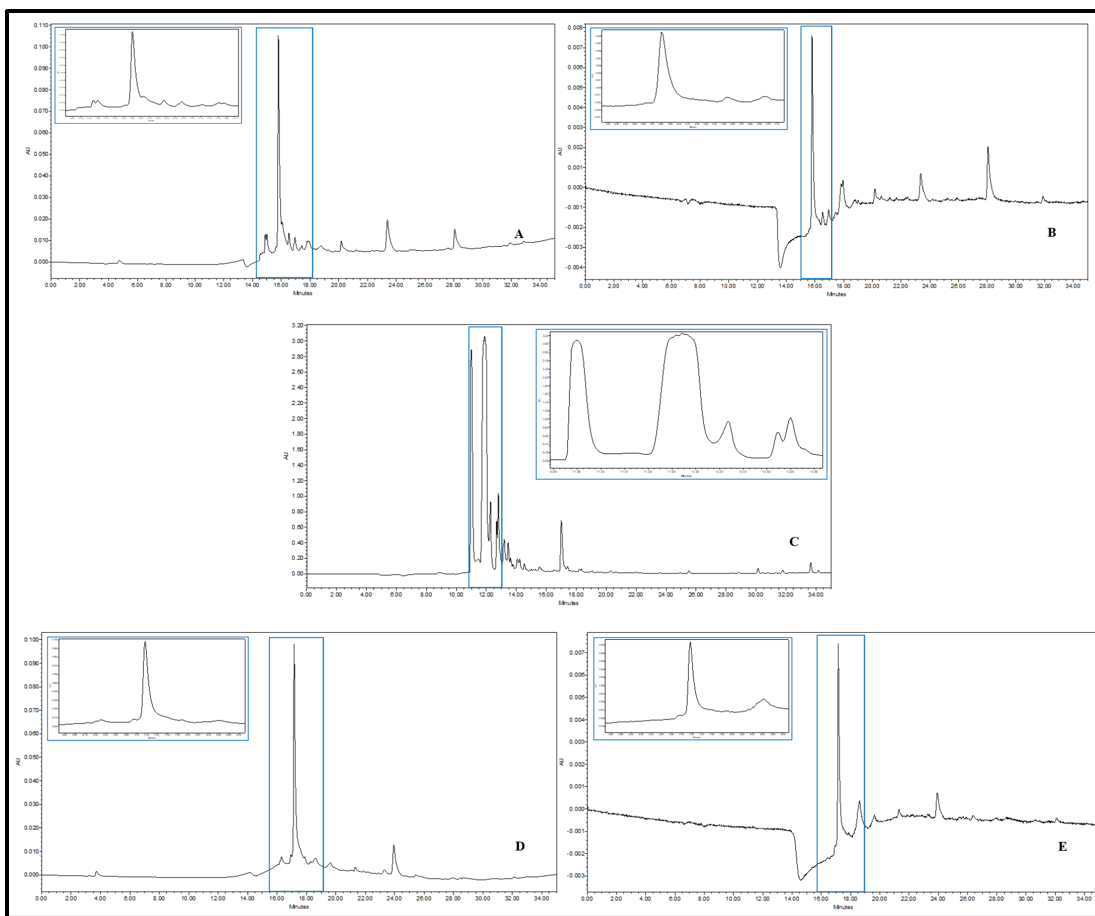


**Figure 3-1. Analytical and Semipreparative RP-HPLC chromatograms of pTatL through the purification process.**

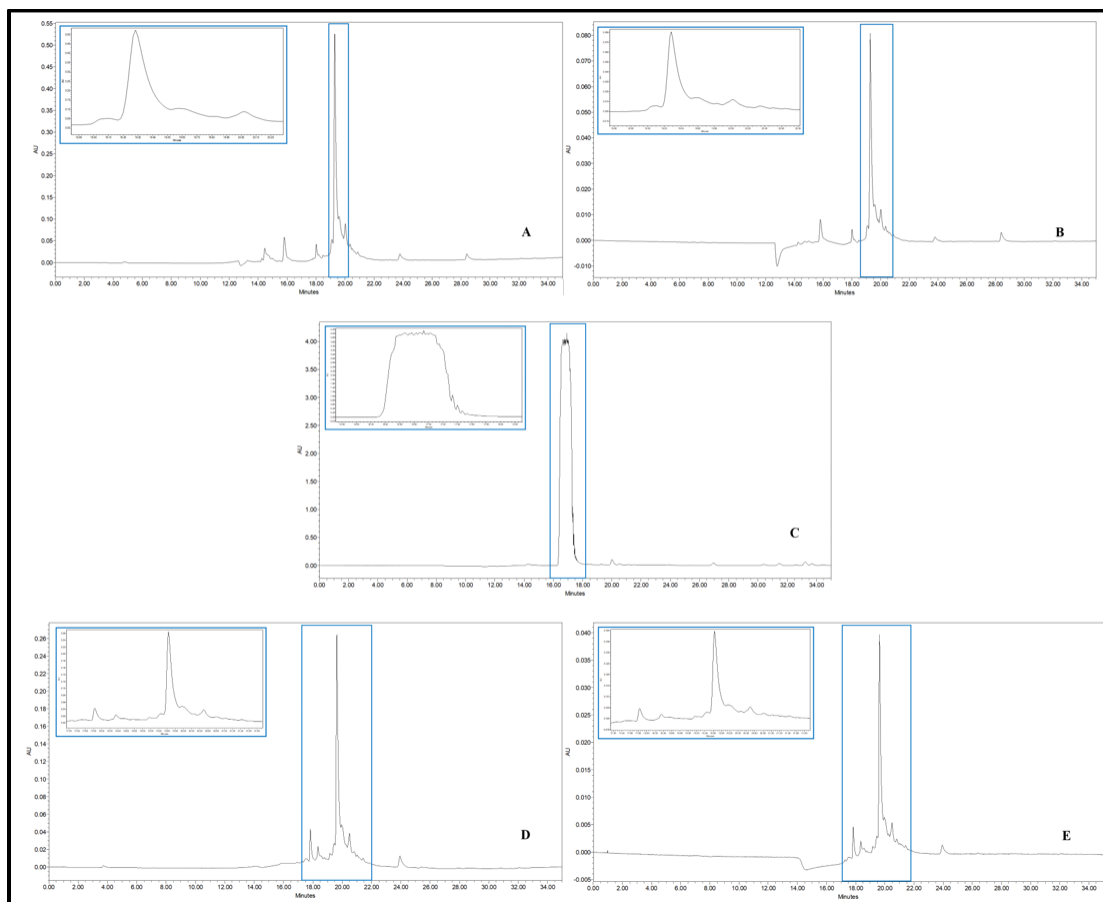
Panels A and B display the analytical chromatograms for the crude pTatL samples detected at 220 nm and 275 nm respectively. Panel C displays the semipreparative chromatogram for the crude pTatL detected at 220 nm. Panels D and E display the analytical chromatograms for the purified pTatL samples detected at 220 nm and 275 nm respectively. The inset image in each panel corresponds to the highlighted peaks. A linear elution gradient from 100% water (with 0.05% TFA) to 100% acetonitrile (with 0.05% TFA) was used with both analytical (Luna® Omega 5  $\mu\text{m}$  Polar C18 100  $\text{\AA}$  (4.6 mm x 250 mm)) and semipreparative (Luna® Omega 5  $\mu\text{m}$  Polar C18 100  $\text{\AA}$  (10 mm x 250 mm)) RP-HPLC columns. The flowrate through the analytical column was 0.75 mL/min and 3.00 mL/min through the semipreparative column.

Figure 3-2 displays the corresponding chromatograms for the purification of the pPenL analog via RP-HPLC. The small chromatograms in the top left, are the zoomed in image of the areas within the blue box in the main chromatogram. Figure 3-2 A and B show the results from the analytical RP-HPLC of the crude pPenL peptide, prior to any purification techniques. A is the

analytical chromatogram of pPenL detected at 220 nm and B is detected at 280 nm. Chromatograms A and B are from the same RP-HPLC experiment, with A (220 nm) indicating components of the crude mixture containing peptide bonds and B (280 nm) indicating components of the crude mixture containing tryptophan residues. In both cases, there was a major peak at a retention time of 19.30 minutes corresponding to the peptide of interest (pPenL). Smaller peaks in A and B can be seen, which indicate impurities in the sample or potential artifacts. Semipreparative RP-HPLC was performed to remove these impurities. An example of a chromatogram from the semipreparative RP-HPLC experiment done to purify the pPenL peptide is displayed in Figure 3-2 C. Chromatogram C displays the visual results of the experiment detected at 220 nm, both 220 nm and 280 nm were observed when conducting these experiments with fractions being collected for the peaks that appeared on both chromatograms at the same retention times. It was determined that the peak displayed in C that corresponded to the pPenL was the peak that eluted between 16.50 and 17.12 minutes. This was confirmed by a second round of analytical RP-HPLC which is displayed in Figure 3-2 D and E, which again show the exact same sample but detected at 220 nm and 280 nm respectively. The complete purification of the pPenL peptide was not accomplished after one round of semipreparative RP-HPLC as can be seen by the minor peaks in chromatograms D and E. The purity of the sample was estimated to be 82% pure, this estimation was performed by the Waters HPLC software which compared the area under the major peak at 19.64 minutes to the summation of the area under the peaks in the chromatogram.

In the zoomed in image of chromatogram C in Figure 3-2, on the upper left corner, the top of the peak is plateaued. This is likely due to overloading of the column. 11 mg of crude material in 2.5 mL of water was injected into the column which was well below the theoretical capacity of the column. This overloading of the column is one potential explanation for the purity of the final

sample. If the column is overloaded then the components of the sample may not bind the stationary phase as intended, resulting in less separation.



**Figure 3-2. Analytical and Semipreparative RP-HPLC chromatograms of pPenL through the purification process.**

Panels A and B display the analytical chromatograms for the crude pPenL samples detected at 220 nm and 280 nm respectively. Panel C displays the semipreparative chromatogram for the crude pPenL detected at 220 nm. Panels D and E display the analytical chromatograms for the purified pPenL samples detected at 220 nm and 280 nm respectively. The inset image in each panel corresponds to the highlighted peaks. A linear elution gradient from 100% water (with 0.05% TFA) to 100% acetonitrile (with 0.05% TFA) was used with both analytical (Luna® Omega 5  $\mu\text{m}$  Polar C18 100  $\text{\AA}$  (4.6 mm x 250 mm)) and semipreparative (Luna® Omega 5  $\mu\text{m}$  Polar C18 100  $\text{\AA}$  (10 mm x 250 mm)) RP-HPLC columns. The flowrate through the analytical column was 0.75 mL/min and 3.00 mL/min through the semipreparative column.

The incomplete isolation of peptides pTatL and pPenL resulting in the 88% and 82% purity, respectively, was something noted when conducting the biophysical experiments using these peptides (Table 3-1). In general, peptide purity from >90% to >95% is best for studies focusing on peptide interaction with biological environments, whereas a peptide purity of >85% is appropriate for semi-quantitative biochemistry experiments.<sup>74</sup>

**Table 3-1. Penetratin and Tat peptide analogs used for this study.**

Peptide	Sequence	Native Peptide	Synthetic Origin	Purity	Theoretical Mass (Da)	Measured Mass (Da)
pPenL	Ac-CGRQIKIWFQNRRMKWKKGC-amide	Penetratin	Personally synthesized (current research)	82%	2608.18	2609.16
pPenC	Ac-CGRQIKIWFQNRRMKWKKGC-amide [disulfide bond 1-20]	Penetratin	Personally synthesized (current research)	Not Purified	2606.16	N/A
pTatL	Ac-CGYGRKKRRQRRRGC-amide	Tat peptide	Personally synthesized (current research)	88%	1921.28	1922.25
pTatC	Ac-CGYGRKKRRQRRRGC-amide [disulfide bond 1-15]	Tat peptide	Personally synthesized (current research)	Not Purified	1919.26	N/A
Pen2	Ac-RQIKIWFQNRRMKWKK-amide	Penetratin	Previously synthesized (An Le) (similar research)	Unknown (>90%)	2287.8	2288*

\*The mass of Pen2 was measured previously by An Le<sup>30</sup>

### 3.2 Use of Dithiothreitol in sample preparation and vesicle preparation

Peptides of varying concentrations in buffer were added to 1 mM PC/PG and PE/PG lipid vesicles in the presence and absence of DTT. Upon addition of the peptide solution to the lipid vesicles, in the absence of DTT, white precipitate could be seen. The precipitation was only seen when pPenL and pTatL were added to the lipid systems, not when the Pen2 peptide was introduced to the vesicles. The amino acid sequences of the penetratin analogs, pPenL and Pen2, are identical except for the additional N- and C-terminal cysteine and glycine residues of pPenL (Table 3-1).

The N- and C-terminal cysteine and glycine residues are also present in the pTatL sequence (Table 3-1). That the precipitation formed only in the presence of the free thiol containing peptides led to the hypothesis that the precipitation was caused by the free thiol groups. The exact interaction of the free thiol groups causing the precipitation was not determined but was believed to be due to peptide oligomers formed through disulfide bonds of the free thiol groups which interacted with the phospholipid vesicles or the free thiol groups directly interacting with the vesicles.

A reducing agent (DTT) was added to the buffers and lipid systems at a final concentration of 1 mM. To maintain the consistent buffer systems inside and outside of the lipid vesicles, the DTT was included in the buffer used to swell the lipid vesicles. Disulfide bonds are reduced in the presence of DTT, and the formation of future disulfide bonds is prevented. The addition of the reducing agent to the buffer and lipid systems resulted in no precipitation occurring after mixing the samples containing 1 mM lipid vesicles with 10 or 20  $\mu$ M peptides. Precipitation did occur in the presence of 1 mM DTT in the 100  $\mu$ M peptide samples. The precipitation in the samples containing the higher concentrations of peptide was not explored further, as the previous studies of Pen2 conducted in the lab resulted in the formation of precipitation when the concentration of peptide surpassed 20  $\mu$ M in lipid environments. The peptide-lipid mixtures are displayed in Figure 3-3 in the absence (A, C) and presence (B, D) of DTT.

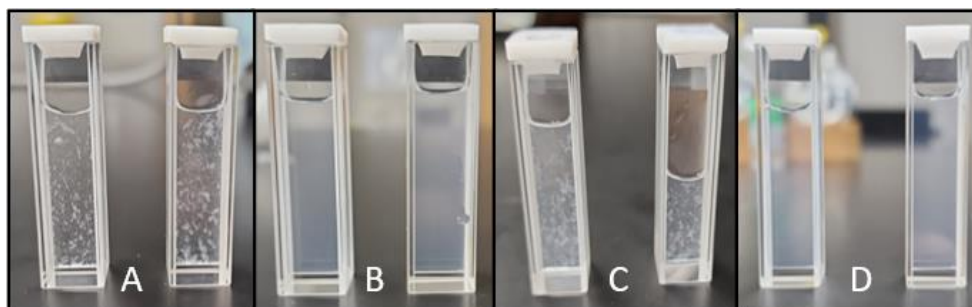


**Figure 3-3. Peptide-lipid vesicle mixtures in the presence and absence of dithiothreitol.**

Peptides of varying concentrations [20  $\mu$ M pPenL (Panel A and B) and 10  $\mu$ M pTatL (Panel C and D) in buffer were mixed in PC/PG and PE/PG lipid vesicles in the presence and absence of dithiothreitol (DTT). 1 mM PCPG systems are in the left cuvette of each panel, and 1 mM PE/PG systems are in the right. Precipitation can be seen in Panels A and C in the absence of DTT. No precipitation is seen in Panels B and D in the presence of 1 mM DTT.

### 3.3 Fluorescence Emission

#### 3.3.1 pTatL fluorescence in different environments

Fluorescence emission spectra of pTatL excited at 275 nm were measured in buffer and 50% HFIP at varying concentrations. The samples were excited at 275 nm due to the presence of a tyrosine residue in the pTatL sequence.<sup>68,75</sup> Tyrosine residues are not as sensitive to their environment as compared to tryptophan residues. The tyrosine residues also show lower intensity in their fluorescence emission spectra, but their emission intensity can be dependent on their surrounding microenvironment (typically, less polar more intensity).<sup>68,75</sup> Tyrosine residues are still used in measuring protein fluorescence as they can indicate slight conformational changes at the surface which tryptophan residues buried in the hydrophobic core could not.<sup>68</sup> Figure 3-4 displays the fluorescence spectra of pTatL at 20  $\mu$ M and 100  $\mu$ M concentrations in buffer and in buffer containing 50% HFIP. There were no shifts observed in the maximum wavelengths of the emission spectra; all the maxima occurred at a wavelength of 303 nm, as expected. The spectra of the peptide in 50% HFIP environments displayed a greater intensity when compared to the

corresponding peptide spectra in buffer. HFIP is known to enhance the secondary structure of peptides, which is a possible explanation for the increase in fluorescence intensity.<sup>60,62</sup> Structural rearrangements can lead to the enhancement of tyrosine fluorescence, if the tyrosine is separated from a group causing the quenching. In most protein-related cases, tyrosine fluorescence is either quenched by excitation energy transfer to tryptophan or ionization of the residue by neighbouring carboxyl or amino groups.<sup>68</sup> A broad peak, or shoulder, between 335 and 385 nm present in the buffer environment, but not in the presence of HFIP, indicates a conformational change in the peptide in the different environments. There are no tryptophan residues present in the sequence of pTatL, meaning the quenching seen in the absence of HFIP is likely caused by the ionization of the residue from a nearby amino group. There have been cases reported in which tyrosine fluorescence is enhanced in the presence of fluoride ions; this is another potential explanation for the increased intensity in the fluorinated environment.<sup>76</sup>

Samples of 10  $\mu\text{M}$  pTatL were prepared in buffer and buffer containing 50% HFIP, but the intensity was too low to reliably distinguish the spectra from the baseline. Samples (10  $\mu\text{M}$  and 20  $\mu\text{M}$ ) were prepared in the presence of 1 mM PC/PG lipid vesicles and 1 mM PE/PG lipid vesicles, but the results were also inconclusive due to weak signal. These results are displayed in the appendix as Figure A3 and Figure A4.

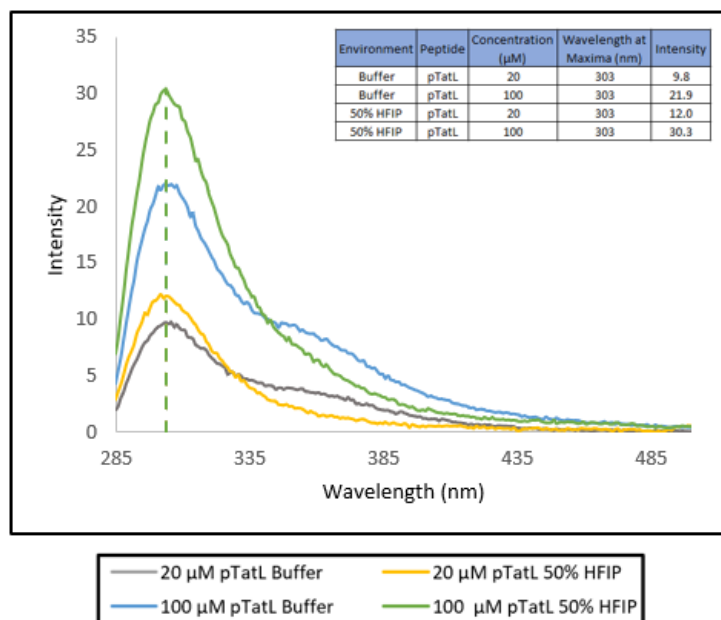


**Figure 3-4. Fluorescence spectra of varying concentrations of pTatL in buffer and 50% HFIP and buffer.** The fluorescence spectra of pTatL were measured in 20 μM and 100 μM concentrations in buffer and in 50% HFIP in buffer. The buffer contained 10 mM Tris-HCl, 150 mM NaCl at pH 7.4. The samples were excited at a wavelength of 275 nm. No shifts were observed in the spectra, as all peaks had their maxima at a wavelength of 303 nm. The spectra of pTatL in buffer (20 μM pTatL is the grey line, 100 μM pTatL is the blue line) display a broader peak with lesser fluorescence intensities than the spectra in the presence of HFIP (20 μM pTatL is the yellow line, 100 μM pTatL is the green line). A right shoulder occurs in both pTatL spectra in the absence of HFIP. The inset tables in each panel display the wavelength at the maxima and the intensity of the maxima of the displayed fluorescence spectra.

### 3.3.2 pPenL fluorescence in different environments

Fluorescence emission spectroscopy measurements of pPenL were used to observe changes in secondary structure as the peptide interacted with different environments. The fluorescence spectra of pPenL in different environments are shown in Figure 3-5; panels A and B display the spectra of 10 μM and 20 μM pPenL, respectively. A change in the fluorescence intensity can be seen in all cases, with the most drastic differences occurring when the peptide in buffer (red) was compared to the peptide in buffer containing 50% HFIP (dark blue). No shift in wavelength could be seen when comparing the maxima of pPenL in the buffer and 50% HFIP spectra as the maxima

of both spectra occur at 356 nm. A shift in the maximum wavelength band was seen when comparing the buffer environment to the PC/PG (yellow) and PE/PG (light blue) lipid vesicles. In each case, the maximum wavelength shifted to a shorter wavelength in the lipid environment indicating a blue-shift. Blue-shifts in the fluorescence spectra of tryptophan show that the tryptophan residues of the peptides are interacting with the more hydrophobic or less polar environments than the tryptophan residues of the peptide in buffer.<sup>32,65,67</sup> The PC/PG spectra were slightly more blue-shifted than the PE/PG spectra with maximum wavelength bands at 346 nm and 349 nm, respectively. The slight shift in the maximum wavelength bands in the PC/PG and PE/PG systems could be due to the two tryptophan residues of pPenL, W8 and W16 being in different environments. In the PC containing lipid system, at least one of the tryptophan residues is in a more hydrophobic environment, than the tryptophan residue(s) in the PE system. The choline group of PC is a more hydrophobic and larger than the ethanolamine group of PE.<sup>24</sup>

The wavelengths at which the maximum of each spectra occurred remained constant when the concentration of the peptide was increased from 10  $\mu\text{M}$  to 20  $\mu\text{M}$  (and 100  $\mu\text{M}$  shown in later figures) in all systems. HFIP was reported to enhance the secondary structure of peptides and interact with the hydrophobic regions of the  $\alpha$ -helices and  $\beta$ -sheets in a way that mimics the negatively charged phospholipids in the lipid membranes.<sup>60</sup> This interaction was not observed in the presence of 50% HFIP; the spectra were not blue-shifted as they were with the lipid systems (Fig. 3-5).

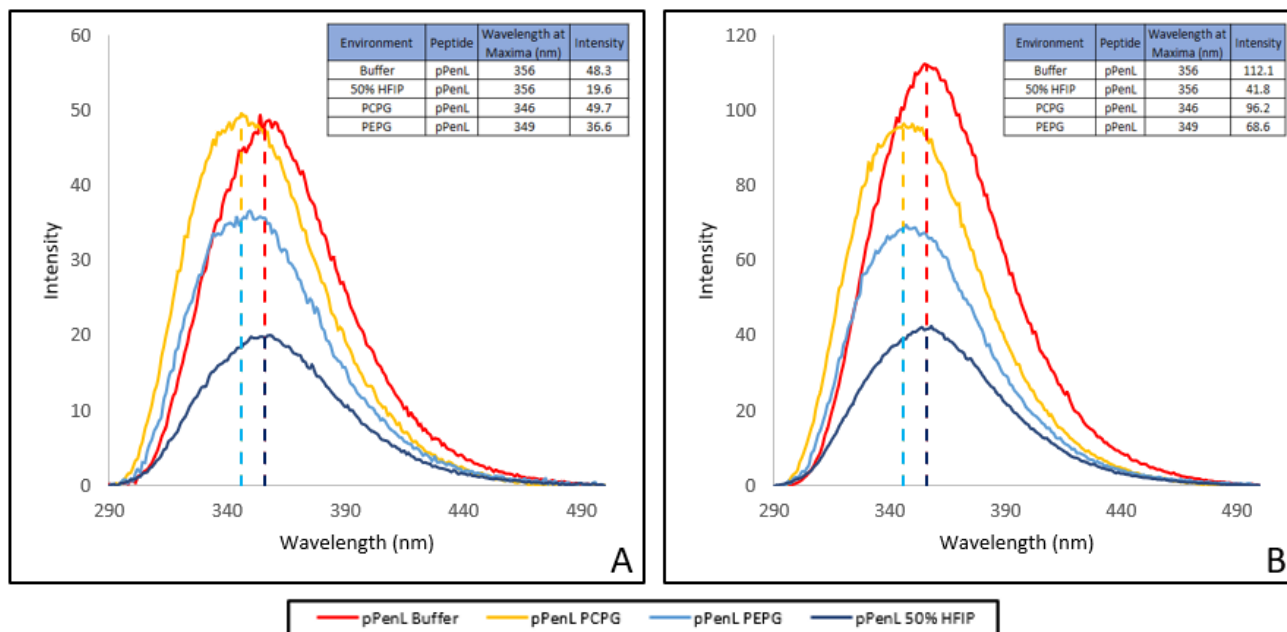


**Figure 3-5. Fluorescence spectra of varying concentrations of pPenL in different environments excited at 280 nm.**

The fluorescence spectra of pPenL were measured in four different environments: buffer (red lines), 50% HFIP in buffer (dark blue), 1 mM PC/PG lipid vesicles (yellow), and 1 mM PE/PG lipid vesicles (light blue). The buffer contained 10 mM Tris-HCl, 150 mM NaCl at pH 7.4. The samples were excited at a wavelength of 280 nm. The spectra of the peptide in lipid vesicle environments all had a slight blue shift, which can be seen by comparing the vertical dotted lines corresponding to the wavelength at which each spectrum's maximum intensity occurs. Panel A shows the spectra of 10 μM pPenL in the different environments and Panel B shows the spectra of 20 μM pPenL.

The inset tables in each panel display the wavelength at the maxima and the intensity of the maxima of the displayed fluorescence spectra.

### 3.3.3 Effect of cysteine on the fluorescence emission of penetratin analogs

The fluorescence spectra of pPenL and Pen2 were measured in different environments to observe the effect that cysteine has on the fluorescence of the penetratin analogs. As previously discussed, and shown in Table 3-1, the difference in sequence between the penetratin analogs (pPenL and Pen2) is the additional glycine and cysteine terminal residues of pPenL. Cysteine is a known quencher of tryptophan fluorescence; cysteine is said to scavenge an electron from the indole ring of the tryptophan residue resulting in a lower fluorescence intensity.<sup>32</sup> The W16 tryptophan residue is more likely to be quenched by cysteine than the W8 tryptophan residue as it

is closer to a cysteine residue in the sequence. It is also possible that the tryptophan fluorescence of one peptide monomer is being quenched by a cysteine residue from a separate peptide monomer in solution. The fluorescence spectra of varying concentrations of the peptides in buffer (Figure 3-6) and in the PC/PG and PE/PG lipid environments (Figure 3-7) were obtained by exciting the peptides at 280 nm. Varying concentrations (10  $\mu\text{M}$ , 20  $\mu\text{M}$ , and 100  $\mu\text{M}$ ) of peptides were used when measuring the fluorescence spectra in buffer. The low concentrations of the peptides (10  $\mu\text{M}$  and 20  $\mu\text{M}$ ) were used in the lipid systems, as precipitation occurred when working with 100  $\mu\text{M}$  concentrations of peptide.

Panels A, B and C of Figure 3-6 display the fluorescence spectra of the peptides at concentrations of 10  $\mu\text{M}$ , 20  $\mu\text{M}$ , and 100  $\mu\text{M}$ , respectively. The data sets in red represent the emission spectra of pPenL and the gold sets represent Pen2. There were no differences observed between the cysteine-containing peptide analog (pPenL) and the peptide without cysteine (Pen2), other than a large difference in intensity. The intensity of the fluorescence spectra of pPenL was lower than that of Pen2 for the 10  $\mu\text{M}$  and 20  $\mu\text{M}$  samples. This was expected as the cysteine residues quench the fluorescence of the tryptophan residues. The 100  $\mu\text{M}$  samples displayed surprising results as the intensity of the pPenL fluorescence spectra had a higher maximum than that of Pen2. This could be explained by the self-aggregation of Pen2 at higher concentrations that was observed in previous experiments by An Le.<sup>30</sup> Self-association of the pPenL monomers at higher concentrations could involve interaction between the tryptophan residues which can protect them from direct quenching by cysteine, and therefore explain the higher fluorescence intensity at 100  $\mu\text{M}$ .<sup>30,32</sup>

Similar results were observed when measuring the fluorescence spectra of pPenL and Pen2 in the lipid environments (Figure 3-7). There were no shifts observed in the maximum wavelengths

when comparing pPenL and Pen2. The decrease in intensity of the Pen 2 spectra, when compared to the pPenL spectra, were also observed.

The differences in intensity, but lack of shift in the spectra's maximum wavelengths suggests that the addition of cysteine and glycine did not significantly alter the peptide structure when comparing pPenL and Pen2 regarding the location of the tryptophan residues in the sequence and the types of environments they are exposed to. Self-association of the pPenL monomers is believed to occur in aqueous and PC/PG systems with increasing concentration of the peptide, as the relative fluorescence intensities were seen to increase when increasing from 10  $\mu\text{M}$  to 20  $\mu\text{M}$ . This increase in fluorescence intensity, as previously mentioned, could be due to the interaction between tryptophan residues in the self-associating peptides protecting them from the direct quenching by cysteine.

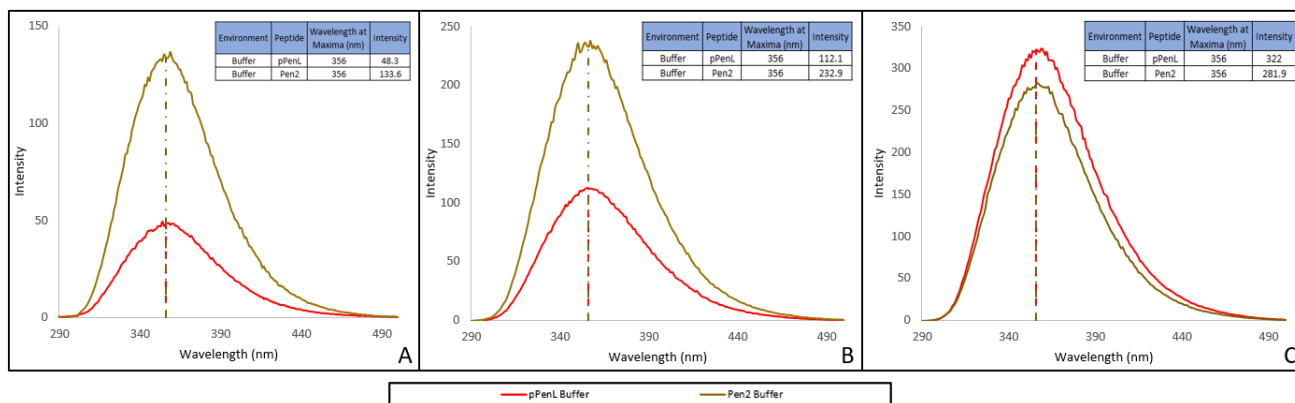


**Figure 3-6. Fluorescence spectra of varying concentrations of pPenL and Pen2 in buffer.**

The fluorescence spectra of pPenL (red) and Pen2 (gold) were measured in buffer (Table 2-1) in varying concentrations to observe the effect of the extra glycine and cysteine residues in the pPenL sequence. Panels A, B and C show the fluorescence spectra excited at 280 nm when the peptides had a concentration of 10  $\mu\text{M}$ , 20  $\mu\text{M}$  and 100  $\mu\text{M}$  respectively. The inset tables in each panel display the wavelength at the maxima and the intensity of the maxima of the displayed fluorescence spectra.

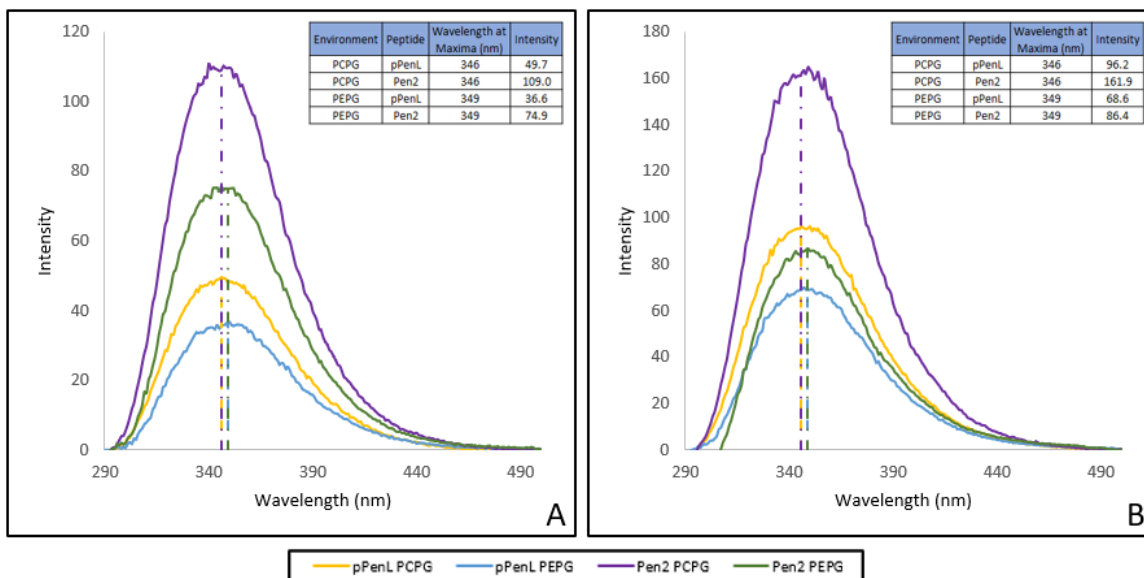


**Figure 3-7. Fluorescence spectra of varying concentrations of pPenL and Pen2 in PC/PG and PE/PG lipid systems.**

The fluorescence spectra of pPenL and Pen2 were measured in the presence of two lipid vesicle systems, 1 mM PC/PG (pPenL is the yellow spectra and Pen2 is the purple spectra) and 1 mM PE/PG (pPenL is the blue spectra and Pen2 is the green spectra) (Table 2-1) in varying concentrations to observe the effect of the extra glycine and cysteine residues in the pPenL sequence. No shifts were observed between the two peptides in the same environment, but as seen previously there was a slight blue-shift when the peptides were measured in the PC/PG vesicles compared to the PE/PG vesicles. Panels A and B show the fluorescence spectra excited at 280 nm when the peptides had a concentration of 10 μM and 20 μM respectively.

The inset tables in each panel display the wavelength at the maxima and the intensity of the maxima of the displayed fluorescence spectra.

### 3.3.4 Effect of fluorine on the fluorescence emission

The fluorescence spectrum of pPenL was measured at several concentrations and in different environments to observe the effect, if any, that fluorine has on the fluorescence of the peptide. Fluoride or chloride ions were present in the buffers used in fluorescence and CD experiments. Both elements are members of the halogen group of elements on the periodic table; a group which contains common tryptophan quenchers such as iodine and bromine.<sup>32</sup> Lighter halogen ions, such as fluoride and chloride are not known to quench fluorescence as efficiently as

the heavier halogen ions, bromide and iodide, but have been reported to quench fluorophores in certain instances.<sup>32</sup> Fluorinated alcohols have also been reported to quench tryptophan fluorescence.<sup>62</sup> Panels A, B and C of Figure 3-8 display the fluorescence spectra of the peptides in 10  $\mu$ M, 20  $\mu$ M, and 100  $\mu$ M concentrations, respectively.

To observe the effect of fluoride and chloride ions, the fluorescence spectra of pPenL were measured in fluorescence buffer containing sodium chloride (red) and in the CD buffer containing sodium fluoride (green). There were no differences observed in the maximum wavelengths when comparing the spectra in the two buffer systems. A small decrease in intensity was seen in the 10  $\mu$ M samples when the chloride containing buffer was compared to the fluoride containing buffer. The difference in intensity decreased as the peptide concentration increased.

To observe the effect of fluorinated alcohol, the fluorescence of pPenL was measured in buffer containing 50% HFIP (dark blue) or 50% IsoP (orange). The fluorinated alcohol environment (HFIP) resulted in a significantly quenched fluorescence spectrum. There was no shift in maximum wavelength in the fluorinated system when compared to either buffer system as they all had their maxima at a wavelength of 365 nm when excited at 280 nm. The nonfluorinated alcohol isopropanol (IsoP) caused a slight blue-shift as the maxima occurred at a wavelength of 351 nm at all concentrations of peptide. This shift indicates that the alcohol influences the polarity of the microenvironment around the tryptophan residues by making it less polar, where in the fluorinated alcohol system the tryptophan residues adapt water like in the buffer environments. The IsoP system also resulted the highest fluorescence intensity. The fluorescence from L-tryptophan in the presence and absence of the fluorinated alcohol was also measured (Figure 3-9) to verify that the quenching observed in the pPenL spectra in Figure 3-8 was solely due to the quenching of the tryptophan residues and not the interaction between the peptide and the HFIP.<sup>60,62</sup>

Fluorinated alcohols, such as HFIP, have been reported to enhance the secondary structure of peptides, and interact with the hydrophobic sections of  $\alpha$ -helical and  $\beta$ -sheet regions of peptides. These potential interactions were not seen to impact the fluorescence emission spectra of pPenL as no shifts were observed in the maxima.

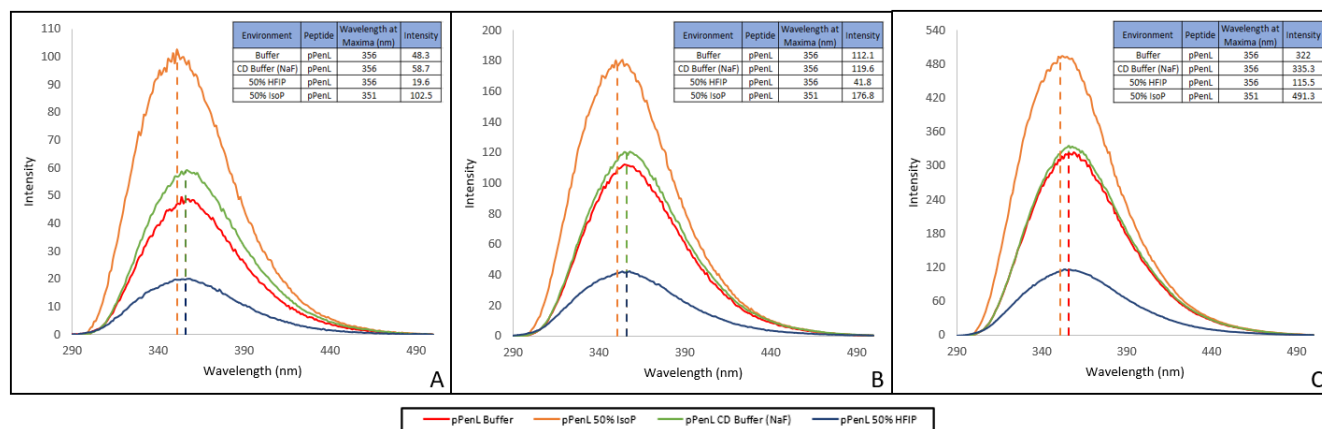


**Figure 3-8. Fluorescence spectra of varying concentrations of pPenL in different buffer and organic environments to observe the effect of fluoride and fluorinated alcohols.**

The fluorescence spectra of varying concentrations of pPenL were measured in four different environments: buffer (red lines), CD buffer (green lines), 50% HFIP in buffer (dark blue), and 50% IsoP in buffer (orange). A slight blue-shift was observed in the 50% IsoP environment that was not seen in the other three environments. Panels A, B and C show the fluorescence spectra excited at 280 nm when the peptides had a concentration of 10  $\mu$ M, 20  $\mu$ M and 100  $\mu$ M respectively. The inset tables in each panel display the wavelength at the maxima and the intensity of the maxima of the displayed fluorescence spectra.

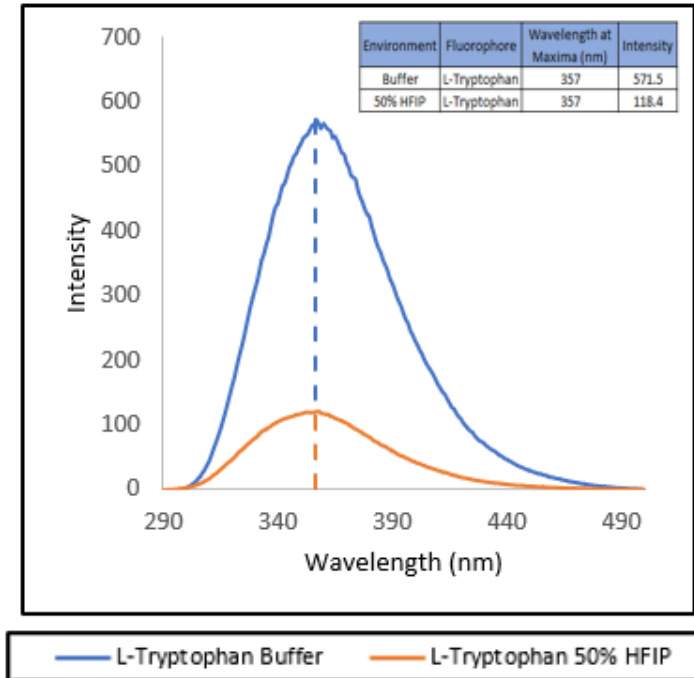


**Figure 3-9. Fluorescence spectra of L-tryptophan in buffer and 50% HFIP and buffer.**

The fluorescence spectra of 100  $\mu$ M L-tryptophan were measured in the absence and presence of HFIP. The fluorescence spectra of pPenL were measured in four different environments: buffer (red lines), 50% HFIP in buffer (dark blue), tryptophan in 50% HFIP in buffer (orange lines), showed a significant decrease in fluorescence intensity when compared to the fluorescence spectrum of the tryptophan in the buffer without the fluorinated alcohol (blue lines). The buffer contained 10 mM Tris-HCl, 150 mM NaCl at pH 7.4. The samples were excited at a wavelength of 280 nm.

The inset tables in each panel display the wavelength at the maxima and the intensity of the maxima of the displayed fluorescence spectra.

### 3.4 Circular Dichroism Spectroscopy

#### 3.4.1 pTatL in different environments

The secondary structures of pTatL were determined in buffer and 50% HFIP/buffer using CD spectroscopy (Figure 3-10). The spectrum of pTatL in buffer (purple) indicates that the peptide has an unordered/random coiled secondary structure due to the large negative minimum around 198 nm and the broad, shallow positive maximum around 224 nm.<sup>55</sup> This result agrees with the unordered secondary structure of the native Tat peptide described in the literature.<sup>13,27,28</sup> In the

presence of 50% HFIP (red) the spectra of pTatL looks to shift to a more  $\alpha$ -helical conformation with the minimum peak around 205 nm. There are shoulders in the largely negative minimum peak that correspond to the expected minima of unordered structures (near 198 nm) and  $\alpha$ -helical structures (near 222 nm) indicating that pTatL in the 50% HFIP environment contains a mixture of unordered and  $\alpha$ -helical secondary structures.<sup>55</sup> This result was not expected as the secondary structure of the native Tat peptide has been reported to remain unordered in different environments and also when conjugated to other molecules.<sup>13,27,28</sup> This indicates that the addition of the terminal cysteine and glycine residues may play a part in the change in conformation of the peptide in the presence of the fluorinated alcohol, HFIP.

Samples of 10  $\mu$ M pTatL were prepared in buffer and 50% HFIP/buffer, but the intensity was too low to reliably distinguish the spectra from the baseline. Samples were prepared in the presence of 1 mM PC/PG lipid vesicles and 1 mM PE/PG lipid vesicles, but the results were also inconclusive. These results are displayed in the appendix as Figure A5.

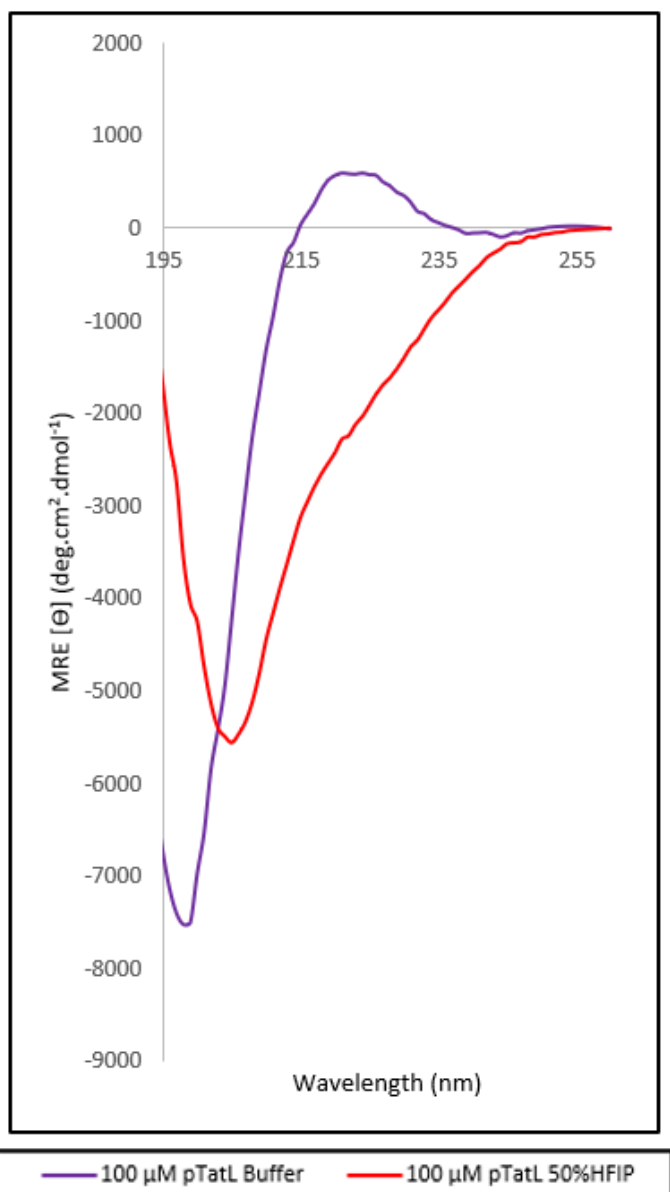


**Figure 3-10. CD spectra of pTatL in buffer in the absence and presence of 50% HFIP.**

Samples of pTatL were prepared in 100  $\mu\text{M}$  concentrations in different environments, then analyzed using far-UV CD spectroscopy at room temperature. The buffer contained 10 mM Tris-HCl, 150 mM NaF at pH 7.4. The spectra of pTatL in buffer (purple) indicates that the peptide has an unordered/random coiled secondary structure due to the large minimum around 198 nm and the broad, shallow maxima around 224 nm. In the presence of 50% HFIP (red) the spectra of pTatL looks to shift to a more  $\alpha$ -helical conformation with the minimum peak around 205 nm.

### 3.4.2 pPenL in different environments

The secondary structures of pPenL were determined in buffer, 50% HFIP/buffer and in the presence of lipid vesicles using CD spectroscopy (Figure 3-11). Figure 3-11 A shows the samples in the buffer solutions in the presence (10  $\mu$ M in the red lines and 100  $\mu$ M in the yellow lines) and absence (10  $\mu$ M in the blue lines and 100  $\mu$ M in the grey lines) of 50% HFIP. In the buffer environment, pPenL displays a mainly unordered conformation with the negative minimum around 200 nm, and the broad, shallow positive maximum near 224 nm.<sup>55</sup> Possible  $\alpha$ -helical secondary structure is evident by the right shoulder of the spectra with small minima between 205 nm and 215 nm.<sup>55</sup> The unordered structure of pPenL in buffer was expected as that is what has been reported in the literature as the secondary structure of the native penetratin peptide.<sup>10,30</sup> In the presence of 50% HFIP, pPenL takes on a mainly  $\alpha$ -helical secondary structure, with the largely negative minimum around 206 nm and the smaller negative minimum around 223 nm.<sup>55</sup> This  $\alpha$ -helical secondary structure was expected in this environment as HFIP is known to enhance the secondary structure of peptides and the native penetratin peptide has been reported to take on the  $\alpha$ -helical secondary structure in the presence of fluorinated alcohols.<sup>10,30</sup>

Figure 3-11 B shows the samples in the presence of lipid vesicles (PC/PG in light blue and PE/PG in green) and 50% HFIP which has been reported to mimic lipid membranes (red lines).<sup>60,62</sup> In the presence of 50% HFIP in the buffer environment (as discussed earlier) and in the presence of the 1 mM lipid vesicles (PC/PG and PE/PG), pPenL takes on a mainly  $\alpha$ -helical secondary structure, with the intense negative minimum around 206 nm and the smaller negative minimum around 223 nm.<sup>55</sup> This  $\alpha$ -helical secondary structure was expected in this environment as HFIP is known to enhance the secondary structure of peptides and the native penetratin peptide has been reported to take on the  $\alpha$ -helical secondary structure in the presence of fluorinated alcohols.<sup>10,30</sup> It

should be noted that the CD data in the presence of lipids is very noisy, which may be skewing the shape of the spectra and therefore may not be reliable.

Samples of 10  $\mu\text{M}$  pPenL were prepared in the presence of 1 mM PC/PG lipid vesicles and 1 mM PE/PG lipid vesicles, but the results were also inconclusive. These results are displayed in the appendix as Figure A6.

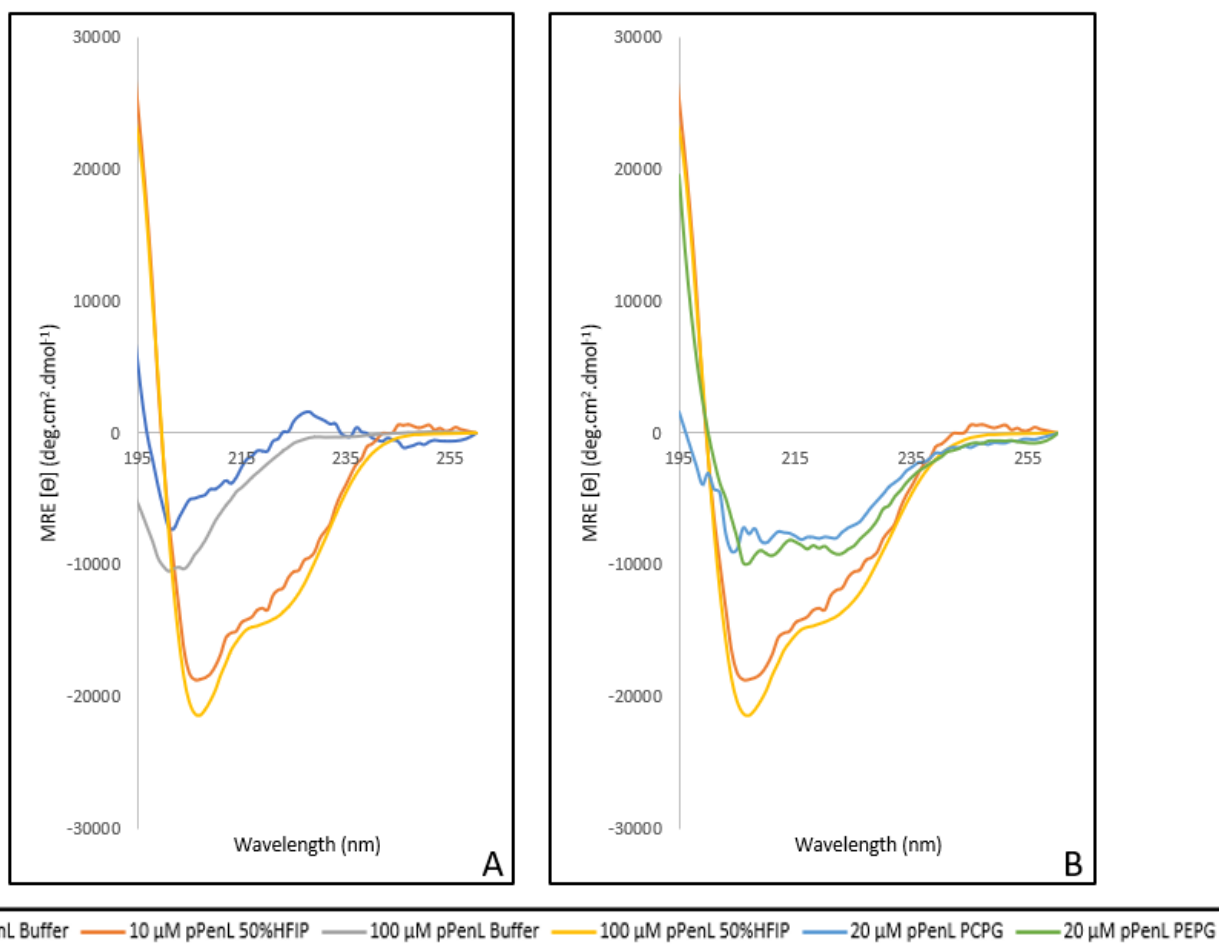


**Figure 3-11. CD spectra of pPenL at different concentrations in buffer environments (buffer with and without 50% HFIP) and in the presence of lipid vesicles and lipid vesicle mimics (PC/PG, PE/PG, and 50% HFIP).**

Samples of pPenL were prepared in varying concentrations in different environments, then analyzed using far-UV CD spectroscopy at room temperature. The buffer contained 10 mM Tris-HCl, 150 mM NaF at pH 7.4. Panel A shows the samples in the buffer solutions in the presence (10  $\mu\text{M}$  in the red lines and 100  $\mu\text{M}$  in the yellow lines) and absence (10  $\mu\text{M}$  in the blue lines and 100  $\mu\text{M}$  in the grey lines) of 50% HFIP. Panel B shows the samples in the presence of lipid vesicles (PCPG in the light blue lines and PEPG in the green lines) and 50% HFIP which has been reported to mimic lipid membranes (red lines).

### **3.5 Isothermal Titration Calorimetry**

ITC experiments were conducted to study the interactions between pPenL and pTatL with PC/PG and PE/PG lipid vesicles. The results of these studies were determined to be inconclusive as the experiments were conducted in the absence of DTT (or other reducing agents). The absence of DTT resulted in the precipitation of the mixed solution of CPP and lipid vesicles, which led to unreliable heat profiles. The experiments were conducted in the absence of DTT under the guidelines from the manufacturer of the isothermal titration calorimeter (MicroCal). Reducing agents, when used in ITC experiments, often result in baseline artifacts or abnormalities which would lead to unreliable final heat profiles.

## Chapter 4: Conclusions

My research project was focused on the synthesis and biophysical analysis of cyclizable analogs of penetratin and the Tat peptide by studying the conformational changes of these peptides when exposed to different environments. The cyclizable analogs, pPenL and pTatL, were synthesized using solid phase peptide synthesis with Fmoc-chemistry. The native peptide sequences were modified to include glycine and cysteine residues at the N and C-termini and protecting the N- and C-termini with acyl and amide groups, respectively. pPenL and pTatL were purified using RP-HPLC resulting in 82% and 88% purity, respectively.

The structure of pPenL changed from unordered in buffer solution to an  $\alpha$ -helical conformation when in the presence of the secondary structure enhancing fluorinated alcohol HFIP and in PC/PG and PE/PG lipid vesicles. The CD and fluorescence spectra for pPenL were comparable to those of the Pen2 peptide, a similar protected penetratin analog without the additional glycine and cysteine residues. Both peptides showed a similar transition from the unordered to  $\alpha$ -helical conformations. The structure of pTatL was unordered in buffer and showed a partial transition to the  $\alpha$ -helical conformation. The native peptide had been reported to maintain its unordered secondary structure when exposed to the different environments, unlike pTatL. These results indicated that the addition of the cysteine and glycine residues to the peptide sequence did not drastically affect the secondary structure or the peptides or how they interact with different environments, except for the precipitation observed when the peptides were incubated in the PC/PG and PE/PG environments.

All experiments were conducted in the presence of a reducing agent, DTT. Precipitation was observed when the peptides were incubated with the PC/PG and PE/PG lipid vesicles in the absence of DTT. The precipitation was not observed in the 10  $\mu\text{M}$  and 20  $\mu\text{M}$  samples of either peptide in the presence of DTT. DTT is not a naturally occurring reducing agent in cell membranes and therefore if the reducing agent is not able to be replaced then these two cyclizable analogs are not suitable for biologically relevant experiments.

Future studies are needed to see if the cyclic versions of these peptides, pPenC and pTatC, can be cyclized and purified. When monitoring the cyclization reaction using UV-Vis spectroscopy at 386 nm to observe the formation of the 5-nitropyridine-2-thiol group, the pH of the solution should also be measured and adjusted if necessary to ensure an appropriate signal can be detected. It is hypothesized that the precipitation of the peptides in the presence of lipid vesicles was due to the free-thiol groups of the peptides' terminal cysteines; if the peptides are successfully cyclized then they will no longer contain free-thiol groups. In this case, there should be no more need of the reducing agent, and the thermodynamics of the interaction between the peptides and the lipid vesicles will be able to be measured.

Further studies could be conducted to determine how the free-thiol groups of the peptides were involved in the precipitation seen in the absence of DTT. Analogs of the penetratin and Tat peptides containing one terminal thiol group instead of two terminal thiol groups could be synthesized to see if free thiols of monomeric linear peptides are interacting with the lipid membranes causing the precipitation or if there is some form of cyclization occurring through the thiol groups leading to the precipitation. Synthesis of the protected analog of the native Tat peptide (the Tat peptide without the addition of the terminal glycine and cysteine residues), would also be beneficial to see if any precipitation forms in the presence of a protected Tat peptide without the

thiol groups. It would also be beneficial to compare the fluorescence and CD results of this peptide to the results of pTatL, in the same way that the pPenL results were compared to the Pen2 results throughout this project.

This research project showed that the modifications to the native peptides done to allow for cyclization did not significantly alter the secondary structure of the peptides when comparing the spectroscopic results. The modifications did not seem to affect the way the analogs interact with the lipid vesicles (in the presence of DTT), with the blue-shifted fluorescence emission spectra and the CD spectra indicating a shift to the  $\alpha$ -helical conformation. Signs of self-association were seen in aqueous and PC/PG environments with increasing concentration of pPenL. The fluorescence intensities began to increase, displaying a decrease in quenching by cysteine. The analog, pPenL, behaving similarly to the original Pen2 peptide, indicates that it may follow the same penetration mechanism. The successful cyclization of these analogs is required in future projects to observe any changes in stability and penetrative ability of the analogs in comparison to their native peptides. This research project along with the suggested future studies could provide key information in the development of the delivery of biologically active cargo across the membrane in a more stable and efficient manner.

## References

- (1) Langel, Ü. *CPP, Cell-Penetrating Peptides*, 1st ed.; Springer Singapore, **2019**.
- (2) Bechara, C.; Sagan, S. Cell-Penetrating Peptides: 20 Years Later, Where Do We Stand? *FEBS Lett.* **2013**, *587* (12), 1693–1702.
- (3) Derakhshankhah, H.; Jafari, S. Cell Penetrating Peptides: A Concise Review with Emphasis on Biomedical Applications. *Biomed. Pharmacother.* **2018**, *108* (September), 1090–1096.
- (4) Joo, S. H. Cyclic Peptides as Therapeutic Agents and Biochemical Tools. *Biomol. Ther.* **2012**, *20* (1), 19–26.
- (5) Gary, S.; Bloom, S. Peptide Carbocycles: From -SS- to -CC- via a Late-Stage “Snip-and-Stitch.” *ACS Cent. Sci.* **2022**, *8* (11), 1537–1547.
- (6) Galande, A. K.; Weissleder, R.; Tung, C. H. An Effective Method of On-Resin Disulfide Bond Formation in Peptides. *J. Comb. Chem.* **2005**, *7* (2), 174–177.
- (7) Gräslund, A.; Madani, F.; Lindberg, S.; Langel, Ü.; Futaki, S. Mechanisms of Cellular Uptake of Cell-Penetrating Peptides. *J. Biophys.* **2011**, *2011*.
- (8) Ruseska, I.; Zimmer, A. Internalization Mechanisms of Cell-Penetrating Peptides. *Beilstein J. Nanotechnol.* **2020**, *11*, 101–123.
- (9) Thorén, P. E. G.; Persson, D.; Isakson, P.; Goksör, M.; Önfelt, A.; Nordén, B. Uptake of Analogs of Penetratin, Tat(48-60) and Oligoarginine in Live Cells. *Biochem. Biophys. Res. Commun.* **2003**, *307* (1), 100–107.
- (10) Magzoub, M.; Graslund, A.; Kilk, K. Interaction and Structure Induction of Cell-Penetrating Peptides in the Presence of Phospholipid Vesicles. *Biochem. Biophys. Acta* **2001**, *1512*, 77–89.
- (11) Wagstaff, K. M.; Jans, D. A. Protein Transduction: Cell Penetrating Peptides and Their Therapeutic Applications. *Front. Med. Chem.* (5) **2012**, 98–126.
- (12) Ziegler, A.; Nervi, P.; Dürrenberger, M.; Seelig, J. The Cationic Cell-Penetrating Peptide CPPTAT Derived from the HIV-1 Protein TAT Is Rapidly Transported into Living Fibroblasts: Optical, Biophysical, and Metabolic Evidence. *Biochemistry* **2005**, *44* (1), 138–148.
- (13) Grunwald, J.; Rejtar, T.; Sawant, R.; Wang, Z.; Torchilin, V. P. TAT Peptide and Its Conjugates: Proteolytic Stability. *Bioconjug. Chem.* **2009**, *20* (8), 1531–1537.
- (14) Vivès, E.; Brodin, P.; Lebleu, B. A Truncated HIV-1 Tat Protein Basic Domain Rapidly Translocates through the Plasma Membrane and Accumulates in the Cell Nucleus. *J. Biol. Chem.* **1997**, *272* (25), 16010–16017.
- (15) Kauffman, W. B.; Fuselier, T.; He, J.; Wimley, W. Mechanism Matters: A Taxonomy of Cell Penetrating Peptides. *Trends Biochem. Sci.* **2015**, *40* (12), 749–764.
- (16) Bagashev, A.; Sawaya, B. E. Roles and Functions of HIV-1 Tat Protein in the CNS: An Overview. *Viol. J.* **2013**, *10*.
- (17) Eguchi, A.; Akuta, T.; Okuyama, H.; Senda, T.; Yokoi, H.; Inokuchi, H.; Fujita, S.; Hayakawa, T.;

- Takeda, K.; Hasegawa, M.; et al. Protein Transduction Domain of HIV-1 Tat Protein Promotes Efficient Delivery of DNA into Mammalian Cells. *J. Biol. Chem.* **2001**, *276* (28), 26204–26210.
- (18) Dupont, E.; Prochiantz, A.; Joliot, A. Penetratin Story: An Overview. *Methods Mol. Biol.* **2015**, *1324*, 29–37.
- (19) Thorén, P. E. G.; Persson, D.; Esbjörner, E. K.; Goksör, M.; Lincoln, P.; Nordén, B. Membrane Binding and Translocation of Cell-Penetrating Peptides. *Biochemistry* **2004**, *43* (12), 3471–3489.
- (20) Prochiantz, A. Messenger Proteins: Homeoproteins, TAT and Others. *Curr. Opin. Cell Biol.* **2000**, *12* (4), 400–406.
- (21) Schneuwly, S.; Klemenz, R.; Gehring, W. J. Redesigning the Body Plan of *Drosophila* by Ectopic Expression of the Homoeotic Gene *Antennapedia*. *Nature*. **1987**, *325* (6107), 816–818.
- (22) Watson, H. Biological Membranes. *Essays Biochem.* **2015**, *59*, 43–70.  
<https://doi.org/10.1042/BSE0590043>.
- (23) Cooper, G.; Hausman, R. *The Cell: A Molecular Approach*, Fourth.; Sinauer Associates: Washington, **2007**.
- (24) Aktas, M.; Danne, L.; Möller, P.; Narberhaus, F. Membrane Lipids in *Agrobacterium Tumefaciens*: Biosynthetic Pathways and Importance for Pathogenesis. *Front. Plant Sci.* **2014**, *5*.
- (25) Akbarzadeh, A.; Rezaei-Sadabady, R.; Davaran, S.; Joo, S. W.; Zarghami, N.; Hanifehpour, Y.; Samiei, M.; Kouhi, M.; Nejati-Koshki, K. Liposome: Classification, Preparation, and Applications. *Nanoscale Res. Lett.* **2013**, *8* (1), 1.
- (26) Eiríksdóttir, E.; Konate, K.; Langel, Ü.; Divita, G.; Deshayes, S. Secondary Structure of Cell-Penetrating Peptides Controls Membrane Interaction and Insertion. *Biochim. Biophys. Acta - Biomembr.* **2010**, *1798* (6), 1119–1128.
- (27) Guo, Q.; Zhao, G.; Hao, F. Effects of the TAT Peptide Orientation and Relative Location on the Protein Transduction Efficiency. *Chem. Biol. Drug Des.* **2012**, *79* (5), 683–690.
- (28) Soo-Jin, L.; Yoon, S. H.; Doh, K. O. Enhancement of Gene Delivery Using Novel Homodimeric Tat Peptide Formed by Disulfide Bond. *J. Microbiol. Biotechnol.* **2011**, *21* (8), 802–807.
- (29) Ren, J.; Zhang, P.; Tian, J.; Zhou, Z.; Liu, X.; Wang, D.; Wang, Z. A Targeted Ultrasound Contrast Agent Carrying Gene and Cell-Penetrating Peptide: Preparation and Gene Transfection in Vitro. *Colloids Surfaces B Biointerfaces* **2014**, *121*, 362–370.
- (30) Le, A. Synthesis and Biophysical Analysis of the Cell-Penetrating Peptide Penetratin and Its Aromatic Analogues, Wilfrid Laurier University, **2020**. MSc Thesis.
- (31) Banerjee, B.; Misra, G.; Ashraf, M. T. *Circular Dichroism*; Elsevier Inc., **2019**.
- (32) Lakowicz, J. R. *Principles of Fluorescence Spectroscopy*, 3rd ed.; Lakowicz, J. R., Ed.; Sp: Baltimore, **2007**.
- (33) Srivastava, V. K.; Yadav, R. *Isothermal Titration Calorimetry*; Elsevier Inc., **2019**.
- (34) Sun, J.; Song, C.; Ma, D.; Shen, S.; Huo, S. Expanding the Toolbox for Peptide Disulfide Bond Formation via I-Methionine Selenoxide Oxidation. *J. Org. Chem.* **2021**, *86* (5), 4035–4044.

- (35) Fourneau, E.; Fischer, E. Ueber Einige Derivate Des Glykocolls. *Ann. d. Chem* **1901**, 276 (134), 2868–2877.
- (36) Stawikowski, M.; Fields, G. B. Introduction to Peptide Synthesis. *Curr. Protoc. Protein Sci.* **2012**, 1 (SUPPL.69), 1–13.
- (37) Grant, G. A. *Synthetic Peptides : A User's Guide*, 2nd ed.; Grant, G. A., Ed.; Oxford University Press, **2002**.
- (38) Tymecka, D.; Misicka, A. Solution Phase Peptide Synthesis: The Case of Biphalin. In *Peptide Synthesis: Methods and Protocols*; Hussein, W., Mariusz, S., Toth, I., Eds.; Humana Press, **2022**; pp 1–12.
- (39) Merrifield, R. B. Solid Phase Peptide Synthesis. I. The Synthesis of a Tetrapeptide. *J. Am. Chem. Soc.* **1963**, 85 (14), 2149–2154.
- (40) Fields, G. B.; Carr, S. A.; Marshak, D. R.; Smith, A. J.; Stults, J. T.; Williams, L. C.; Williams, K. R.; Young, J. D. Evaluation of Peptide Synthesis As Practiced in 53 Different Laboratories. In *Techniques in Protein Chemistry IV*; Elsevier, **1993**; pp 229–238.
- (41) Carpino, L. A.; Han, G. Y. The 9-Fluorenylmethoxycarbonyl Function, a New Base-Sensitive Amino-Protecting Group. *J. Am. Chem. Soc.* **1970**, 92 (19), 5748–5749.  
<https://doi.org/10.1021/ja00722a043>.
- (42) Chan, W. C.; White, P. D. *Fmoc Solid Phase Peptide Synthesis*; Oxford University Press, **2000**.
- (43) Merck. *Novabiochem Peptide Synthesis.*; Merck KGaA: Darmstadt, **2014**.
- (44) Petrou, C.; Sarigiannis, Y. *Peptide Synthesis: Methods, Trends, and Challenges*; Elsevier Ltd, **2017**.
- (45) Hood, C.; Fuentes, G.; Patel, H.; Page, K.; Menakuru, M.; Park, J. Fast Conventional Fmoc Solid-Phase Peptide Synthesis with HCTU. *J. Pept. Sci.* **2007**, No. October 2006, 16–26.
- (46) Guzman, F.; Arostica, M.; Roman, T.; Beltran, D.; Gauna, A.; Albericio, F.; Cardenas, C. Peptides Solid-Phase Synthesis and Characterization Tailor-Made Methodologies. *Electron. J. Biotechnol.* **2023**, 64, 27–33.
- (47) Calce, E.; Vitale, R. M.; Scaloni, A.; Amodeo, P.; De Luca, S. Air Oxidation Method Employed for the Disulfide Bond Formation of Natural and Synthetic Peptides. *Amino Acids* **2015**, 47 (8), 1507–1515.
- (48) Schroll, A.; Hondal, R.; Flemer Jr, S. 2,2'-Dthiobis(5-Nitropyridine)(DTNP) as an Effective and Gentle Deprotectant for Common Cysteine Protecting Groups. *J. Pept. Sci.* **2012**, 18 (1), 1–9.
- (49) Ste.Marie, E.; Hondal, R. Reduction of Cysteine-S-Protecting Groups by Triisopropylsilane. *J. Pept. Sci.* **2018**, 24 (11), 1–17.
- (50) Snyder, L. R.; Kirkland, J. J. *Introduction to Modern Liquid Chromatography*, 2nd ed.; John Wiley and Sons Inc., **1979**.
- (51) Meyer, V. R. *Practical High-Performance Liquid Chromatography: Fourth Edition*; **2006**; Vol. 3.
- (52) Rathore, A. S.; Joshi, S. *Liquid Chromatography | Historical Development*, 3rd ed.; Elsevier Inc., **2019**.

- (53) Aguilar, M. Reversed-Phase High-Performance Liquid Chromatography. *Methods Mol. Biol.* **2004**, 251, 9–22.
- (54) Ong, S. G. M.; Chitneni, M.; Lee, K. S.; Ming, L. C.; Yuen, K. H. Evaluation of Extrusion Technique for Nanosizing Liposomes. *Pharmaceutics* **2016**, 8 (4), 1–12.
- (55) Greenfield, N. J. Using Circular Dichroism Spectra to Estimate Protein Secondary Structure. *Nat. Protoc.* **2007**, 1 (6), 2876–2890.
- (56) Jelokhani-Niaraki, M.; Ivanova, M. V.; McIntyre, B. L.; Newman, C. L.; McSorley, F. R.; Young, E. K.; Smith, M. D. A CD Study of Uncoupling Protein-1 and Its Transmembrane and Matrix-Loop Domains. *Biochem. J.* **2008**, 411 (3), 593–603.
- (57) Zhang, S. Discovery of the First Self-Assembling Peptide, Study of Peptide Dynamic Behaviors, and G Protein-Coupled Receptors Using an Aviv Circular Dichroism Spectropolarimeter. *Biopolymers* **2018**, 109 (8), 1–12.
- (58) Andrews, S. S.; Tretton, J. Physical Principles of Circular Dichroism. *J. Chem. Educ.* **2020**, 97 (12), 4370–4376.
- (59) Sönnichsen, F. D.; Van Eyk, J. E.; Hodges, R. S.; Sykes, B. D. Effect of Trifluoroethanol on Protein Secondary Structure: An NMR and CD Study Using a Synthetic Actin Peptide. *Biochemistry* **1992**, 31 (37), 8790–8798.
- (60) Colomer, I.; Chamberlain, A. E. R.; Haughey, M. B.; Donohoe, T. J. 1,1,1,3,3,3-Hexafluoro-2-Propanol (HFIP): More than a Polar Protic Solvent. *Catal. from A to Z* **2020**, 1–16.
- (61) Buck, M. Trifluoroethanol and Colleagues: Cosolvents Come of Age. Recent Studies with Peptides and Proteins. *Q. Rev. Biophys.* **1998**, 31 (3), 297–355.
- (62) Roccatano, D.; Fioroni, M.; Zacharias, M.; Colombo, G. Effect of Hexafluoroisopropanol Alcohol on the Structure of Melittin: A Molecular Dynamics Simulation Study. *Protein Sci.* **2005**, 14 (10), 2582–2589.
- (63) Mulla, H. R.; Cammers-Goodwin, A. Stability of a Minimalist, Aromatic Cluster in Aqueous Mixtures of Fluoro Alcohol [14]. *J. Am. Chem. Soc.* **2000**, 122 (4), 738–739.
- (64) Chen, Y.; Barkley, M. D. Toward Understanding Tryptophan Fluorescence in Proteins. *Biochemistry* **1998**, 37 (28), 9976–9982.
- (65) Senesi, N.; D’Orazio, V. Fluorescence Spectroscopy. *Encycl. Soils Environ.* **2004**, 4, 35–52.
- (66) Sahoo, H. Förster Resonance Energy Transfer - A Spectroscopic Nanoruler: Principle and Applications. *J. Photochem. Photobiol. C Photochem. Rev.* **2011**, 12 (1), 20–30.
- (67) Vivian, J. T.; Callis, P. R. Mechanisms of Tryptophan Fluorescence Shifts in Proteins. *Biophys. J.* **2001**, 80 (5), 2093–2109.
- (68) Zhdanova, N. G.; Shirshin, E. A.; Maksimov, E. G.; Panchishin, I. M.; Saletsky, A. M.; Fadeev, V. V. Tyrosine Fluorescence Probing of the Surfactant-Induced Conformational Changes of Albumin. *Photochem. Photobiol. Sci.* **2015**, 14 (5), 897–908.
- (69) Kozlov, A. G.; Lohman, T. M. SSB Binding to SsDNA Using Isothermal Titration Calorimetry. *Methods Mol. Biol.* **2012**, No. 922, 37–54.

- (70) Murphy, J.; Knutson, K.; Hinderliter, A. *Protein–Lipid Interactions*, 1st ed.; Elsevier Inc., **2009**; Vol. 466.
- (71) Hevener, K. E.; Pesavento, R.; Ren, J.; Lee, H.; Ratia, K.; Johnson, M. E. Hit-to-Lead : Hit Validation and Assessment. *Methods Enzymol.* **2018**, *610*, 265–309.
- (72) Nichols, M.; Kuljanin, M.; Nategholeslam, M.; Hoang, T.; Vafaei, S.; Tomberli, B.; Gray, C. G.; Debruin, L.; Jelokhani-niaraki, M. Dynamic Turn Conformation of a Short Tryptophan-Rich Cationic Antimicrobial Peptide and Its Interaction with Phospholipid Membranes. *J. Phys. Chem. B* **2013**, *117*, 14697–14708.
- (73) James, N. G.; Mason, A. B. Protocol to Determine Accurate Absorption Coefficients for Iron Containing Transferrins. *Anal. Biochem.* **2009**, *378* (2), 202–207.
- (74) Scientific, T. Peptide Synthesis <https://www.biocompare.com/Editorial-Articles/117894-Peptide-Synthesis/#:~:text=Many analytical applications use mid,purification and testing of antibodies.> Accessed April 14<sup>th</sup>, 2023.
- (75) Guzow, K.; Ganzynkowicz, R.; Rzeska, A.; Mrozek, J.; Szabelski, M.; Karolczak, J.; Liwo, A.; Wiczak, W. Photophysical Properties of Tyrosine and Its Simple Derivatives Studied by Time-Resolved Fluorescence Spectroscopy, Global Analysis, and Theoretical Calculations. *J. Phys. Chem. B* **2004**, *108* (12), 3879–3889.
- (76) Kumar, N.; Mandal, S. K. L-Tyrosine Derived Fluorescent Molecular Probes as Solvent Mediated Flip-Flop Halide (Iodide/Fluoride) Sensors and Reversible Chromogenic PH Indicators. *Mater. Adv.* **2021**, *2* (3), 942–947.

## Appendix

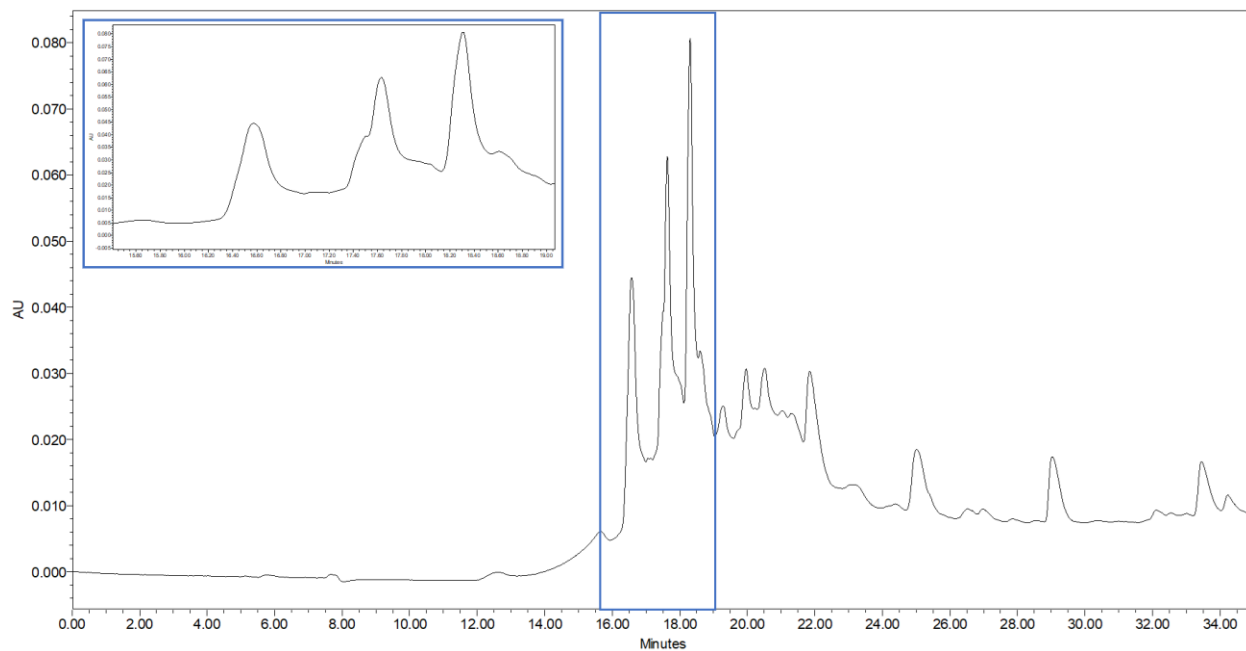


**Figure A1. Analytical RP-HPLC chromatogram of pTatC detected at 220 nm.**

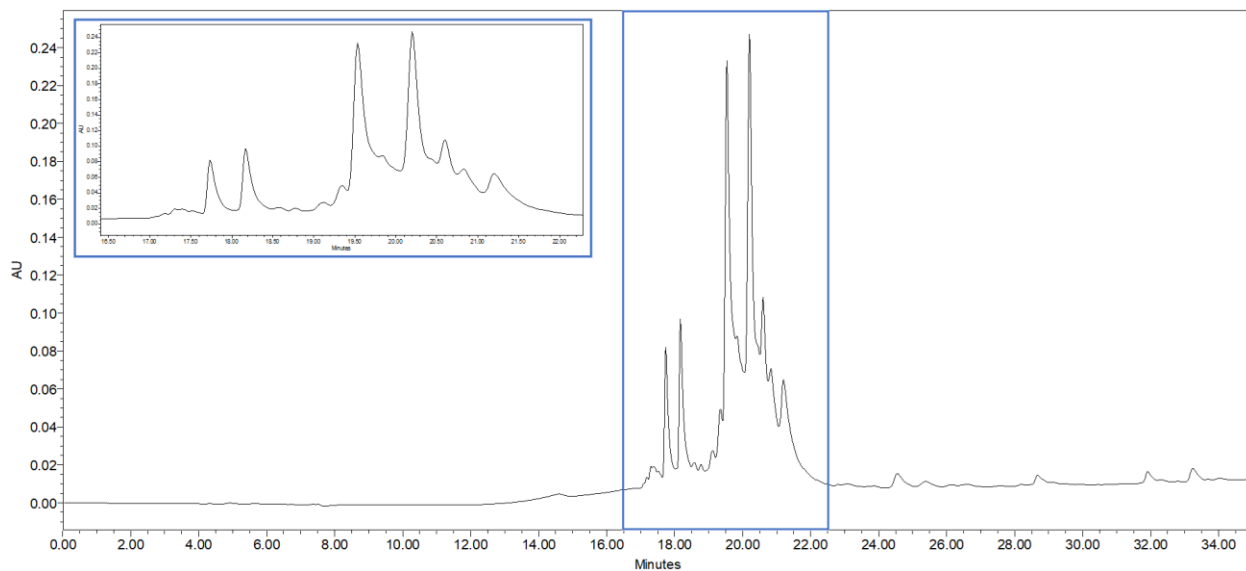


**Figure A2. Analytical RP-HPLC chromatogram of pPenC detected at 220 nm.**

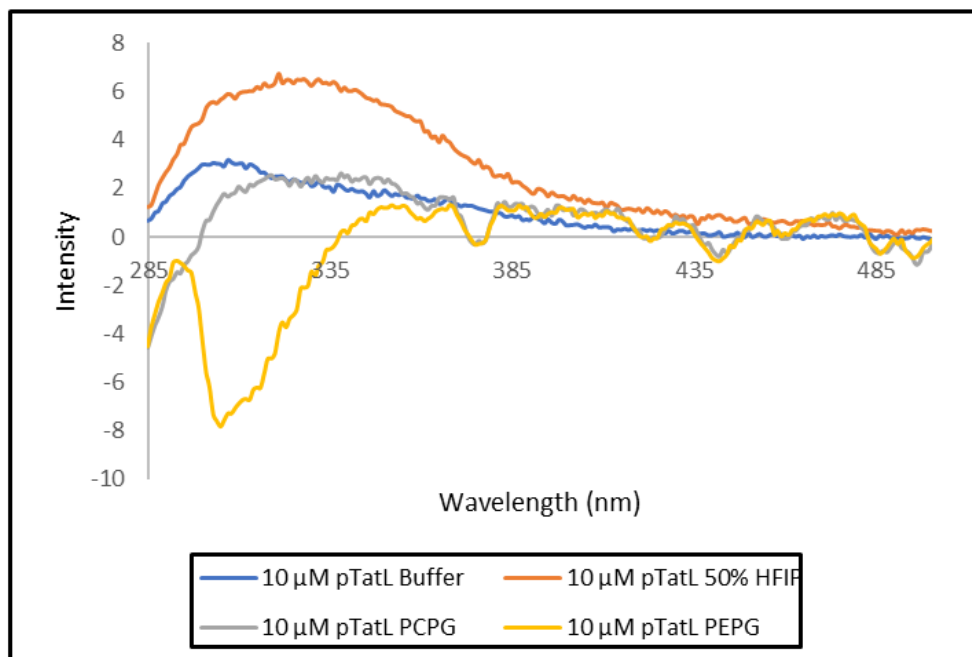


**Figure A3. Fluorescence spectra of 10  $\mu\text{M}$  pTatL in different environments.**

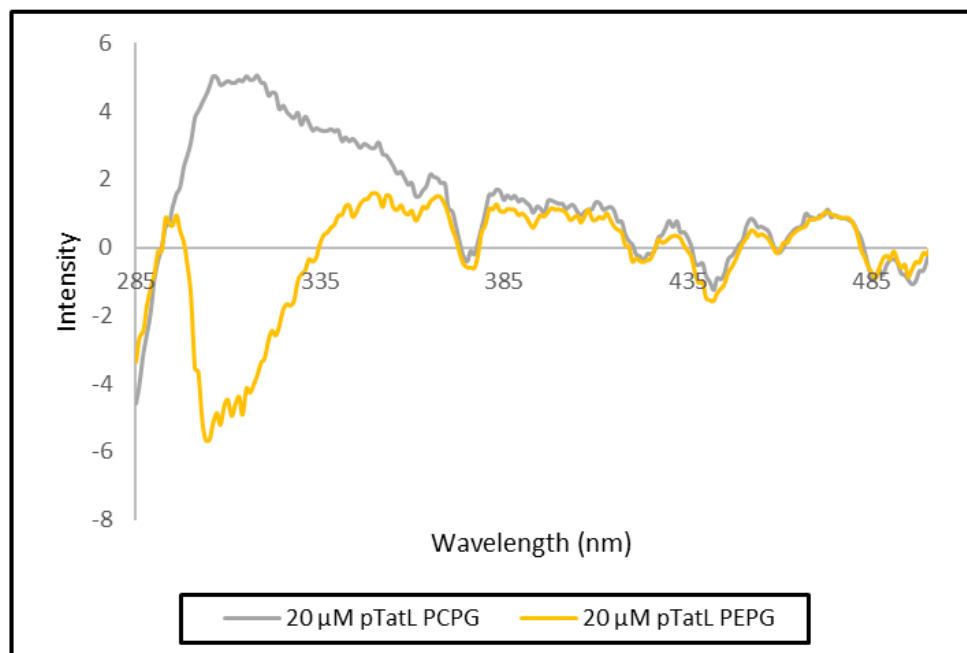


**Figure A4. Fluorescence spectra of 20  $\mu\text{M}$  pTatL in lipid environments.**

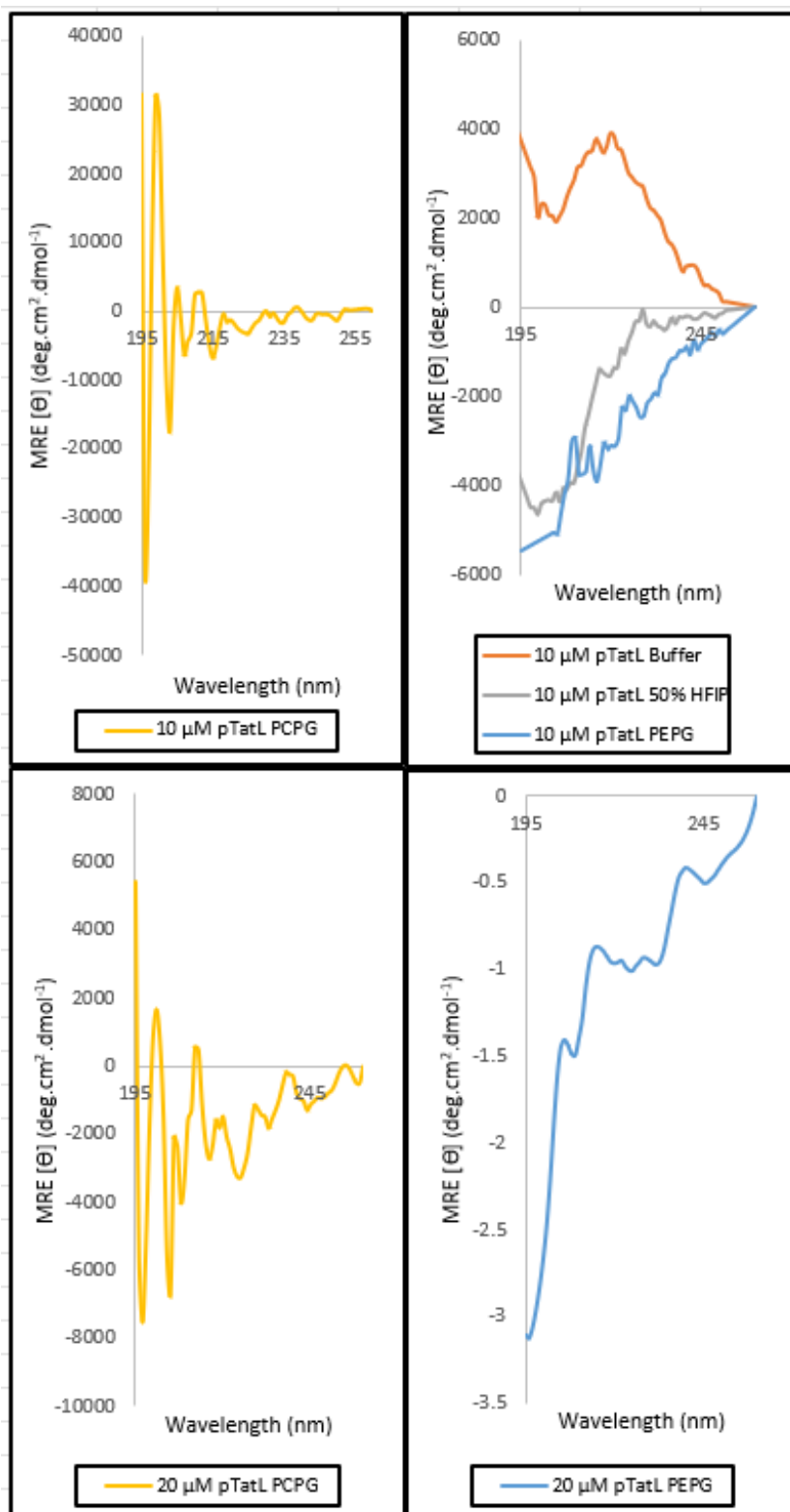


**Figure A5. Inconclusive CD Spectra of pTatL.**

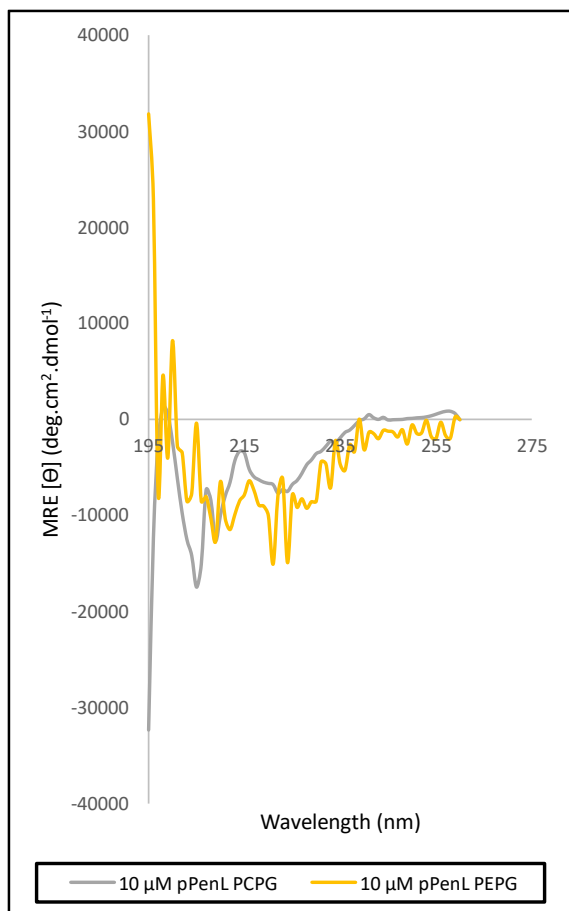


**Figure A6. Inconclusive CD Spectra of 10 μM pPenL in lipid environments.**